LUND UNIVERSITY

Redistribution of moisture and ions in cement based materials

Åhs, Magnus

2011

Redistribution of moisture and ions in cement based materials

Magnus Åhs

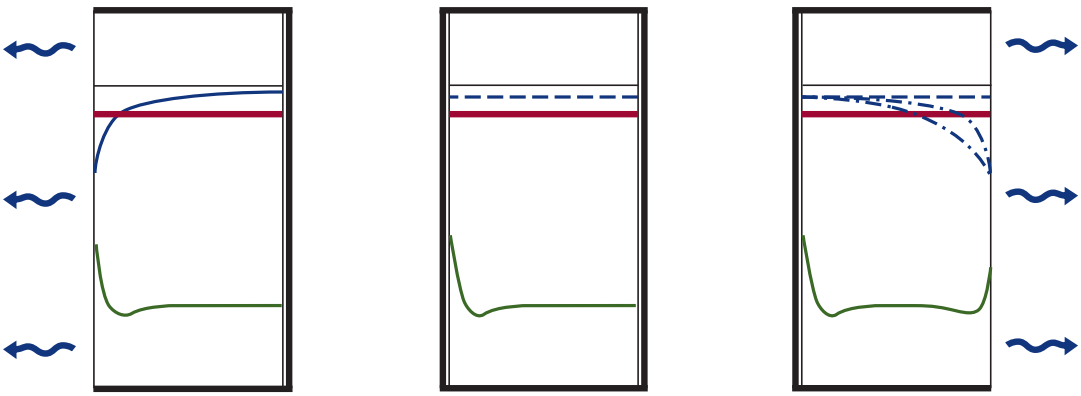

Division of Building Materials
Lund University

Redistribution of moisture and ions in cement based materials

Magnus Åhs

LUND UNIVERSITY

Doctoral Thesis, Report TVBM-1028, Division of Building Materials,
Lund Institute of Technology, Lund University, Lund 2011

ISRN LUTVDG/TVBM--11/1028--SE(1-86)
ISSN 0348-7911 TVBM
ISBN 978-91-7473-126-2

Lund University
Division of Building Materials
P.O. Box 118
SE-221 00 Lund, Sweden

Telephone:+46 46 222 74 15
Telefax:+46 46 222 44 27
www.byggnadsmaterial.lth.se

Preface

This doctoral thesis is the result of six years of research conducted at the division of Building Materials, Lund University. It was funded by SBUF, the Development Fund of the Swedish Construction Industry, FORMAS, the Swedish Research Council for Environment, Agricultural Sciences and Spatial Planning, NCC Construction Sweden, Skanska Sweden, maxit Group AB and Strängbetong AB. A part of this project was a partner project in NanoCem.

I would like to thank my supervisors, Professor Lars-Olof Nilsson and Professor Lars Wadsö at the division of Building Materials, for their encouragement and support throughout this research.

The practical work in this research was performed in cooperation with the technical staff at the division of Building Materials, Stefan Backe, Bo Johansson, Ingemar Larsson and last but definitely not least Bengt Nilsson. Their technical skills and experience simplified the laboratory work. Marita Persson and Britt Andersson, the administrative back bone of the division of Building Materials, have contributed to the completion of my thesis with their organizational skills.

Representatives from the construction industry are hereby acknowledged for their contributions to this work.

All my fellow Ph.D. students are hereby recognized for their contribution to this thesis.

Finally, I would like to express my gratitude to my wife Jessica for her support.

Abstract

There were two principal objectives for this thesis. The first was to develop a methodology and evaluation model of moisture redistribution in order to make the future relative humidity in a screeded concrete slab predictable. The second objective was to develop a method to determine the critical humidity for ion transport in concrete.

Residual moisture in screeded concrete slabs may be redistributed to the top screed surface under a semi-permeable flooring, thus elevating the relative humidity, RH, and possibly exceeding the critical humidity level. Passing the critical humidity level may result in material damage to the flooring and adhesive. In order to avoid such damage there is a need of a methodology to estimate the maximum humidity obtained underneath flooring.

The redistribution of residual moisture may increase the concentration of alkali at the contact area between the adhesive and concrete. This alkali increase may initiate and sustain adhesive deterioration, which is a common moisture related damage.

Several screeded concrete slabs with PVC flooring were prepared to reproduce and monitor moisture distribution and the subsequent redistribution. The moisture distribution before flooring and after a certain period of redistribution is presented. In addition, sorption isotherms including scanning curves were determined in a sorption balance for materials used in the floor constructions, viz, w/c 0.65 concrete, w/c 0.4 concrete, w/c 0.55 cement mortar, and Floor 4310 Fibre Flow, a self levelling flooring compound. Repeated absorption and desorption scanning curves starting from the desorption isotherm were also investigated.

The measurements performed made it possible to develop both a qualitative and quantitative model of moisture redistribution and to quantify the humidity achieved under the flooring. The hysteresis phenomenon of the sorption isotherm is considered in the model.

The model is well suited for estimations of the future RH underneath flooring in a screeded concrete slab and may also be used on homogeneous slabs.

Results from previous research suggested that early drying of the concrete slab can mitigate the increase in relative humidity that occurs when an impermeable floor covering is installed. A study was conducted to verify these results. The results of this new study of the effects of early drying could not demonstrate any significant difference between an early and late dehydration.

The redistribution of ions under different moisture conditions was investigated with a newly developed method. The method is divided into a precondi-

tioning of test specimens and also a method to determine the redistribution of potassium ions. This preconditioning provides a well defined moisture condition of the specimen, which is important for determining the critical humidity for the transport of ions. The redistribution is detected by examining the ion content distribution before and after the preconditioning of ion species already present in the concrete. Previous research in this area has been conducted through adding chloride ions to the specimens. However, redistribution of chloride ions is impeded in that they bind to the inner pore surfaces, which poses a risk that the critical moisture level may be affected/misjudged.

Key words

Moisture redistribution, ion redistribution, cement based materials, sorption isotherm, hysteresis, scanning

Sammanfattning

Nygjuten betong innehåller överskottsfukt som avges till omgivningen under uttorkningen. Om uttorkningen får fortsätta i en konstant luftfuktighet antar betongen så småningom samma fuktighet. Eftersom betong är ett tätt material tar det lång tid, ofta flera år, innan så har skett. Tills detta har inträffat sker en fukttransport från de inre delarna ut till ytan.

En del av överskottsfukten i betongplattor kan omfördelas till golvytan och därmed öka fuktigheten under en tät golvbeläggning. Eventuellt överskrids då den kritiska fuktnivån. I många sammanhang används en tunnare pågjutning för att jämna av ytan för att kunna lägga en golvbeläggning direkt på underlaget. Det här produktionssättet innebär att ny fukt tillkommer genom pågjutningen och omfördelningen av fukt kompliceras. Om den kritiska fuktnivån överskrids kan det leda till materiella skador på golv och lim. Det nya produktionssättet innebär ett behov av att kunna uppskatta den maximala fuktigheten under ett tätt golvmaterial även för pågjutna betongkonstruktioner.

Överskottsfukten innehåller joner från cementet, framför allt kalcium men också mindre mängder kalium och natrium, vilka alla höjer pH i fukten och gör den basisk. Den starkt basiska och fuktiga miljön har en negativ inverkan på många material. Golvlimmet under en PVC-matta är ett material som är känsligt för en sådan miljö. Genom att torka bort en del av överskottsfukten är det möjligt att limma golvmattan utan att riskera att limmet bryts ner.

Med dagens snabba byggtakt är det gynnsamt att torka bort så lite som möjligt av överskottsvattnet, med en viss säkerhetsmarginal, och ändå undvika att en fuktskada uppstår.

Målet med den här doktorsavhandlingen var dels att utveckla en modell och metod för att förutsäga den framtida relativa fuktigheten i en pågjuten betongplatta, och dels att utveckla en metod för att bestämma den kritiska fuktigheten för jontransport i betong.

Omfördelningen av kvarvarande fukt kan också föra med sig alkalijoner och öka koncentrationen i kontaktytan mellan lim och betong. Denna alkaliökning kan tillsammans med den omfördelade fukten initiera och upprätthålla nedbrytning av lim, vilket är en vanligt förekommande fuktrelaterad skada.

Flera pågjutna betongplattor med PVC-matta tillverkades för att skapa och följa fuktfördelningen och efterföljande omfördelning. Fuktfördelningen före golvläggning och efter en viss tid av omfördelning presenteras för de tillverkade betongplattorna. Dessutom bestämdes sorptionsisotermer inklusive scanningkurvor med en sorptionsvåg för materialen som användes, betong med vct 0.65 och vct 0.4 och ett cementbruk med vct 0.55, samt Floor 4310 Fibre Flow, en

självavjämnande golvmassa. Upprepade absorptions- och desorptionsscanningkurvor som startat från desorptionsisotermen bestämdes också.

De utförda mätningarna gjorde det möjligt att utveckla en kvalitativ och kvantitativ modell för fuktomfördelningen och att kvantifiera hur fuktigt det blir under en tät golvbeläggning. Båda modellerna tar hänsyn till inverkan av hysteres. Den kvantitativa modellen lämpar sig väl för bedömningar av den framtida fuktigheten, i % RF, under golv i en pågjuten betongplatta och kan också användas på homogena plattor.

Resultat från tidigare forskning antydde att en tidig uttorkning av betong plattan kan mildra höjningen av relativ fuktighet som sker vid omfördelning under en tät golvbeläggning. En studie genomfördes för att kontrollera dessa resultat. Resultaten från den nya studien av inverkan av tidig uttorkning kunde inte påvisa någon betydande skillnad mellan en tidig eller sen uttorkning.

Uttorkning av betong genererar en fukttransport mot den torkande ytan. Den fukttransporten kan leda till en anrikning av joner vid ytan. Omfördelning av joner vid olika fukttillstånd undersöktes därför med en nyutvecklad metod. Metoden är indelad i en förkonditionering av provkroppar och dels en metod för att mäta omfördelningen av kaliumjoner. Metoden innebär att fukttillståndet i provkroppen blir väldefinierat, vilket är viktigt för att bestämma den kritiska fuktigheten för transport av joner. Dessutom mäts omfördelningen av joner som redan finns i betong. Tidigare forskning på det här området har utförts med hjälp av tillsatta kloridjoner. Transporten av kloridjoner hindras i viss mån att omfördelas genom att de binds till de inre porytorna vilket innebär en risk när den kritiska fuktnivån ska bestämmas.

Papers

This thesis is based on the following papers, which will be referred to in the text by their Roman numerals. The papers are appended at the end of the thesis.

Paper I. Remote monitoring and logging of relative humidity in concrete, Åhs, M., (2005). Proceedings of the 7^{th} Symposium on Building Physics in the Nordic Countries, The Icelandic Building Research Institute, Reykjavik, Iceland, pp 181-187.

Paper II. A method for study sorption phenomena, Åhs, M., Sjöberg, A., Anderberg, A., (2005), Proceedings of the 10^{th} International Conference on Indoor Air Quality and Climate, Beijing, China, pp 1969-1973.

Paper III. Scanning sorption isotherms for hardened cementitious materials, Åhs, M., (2008), Construction and Building Materials, Volume 22, issue 11, pp 2228-2234.

Paper IV. Moisture distribution in screeded concrete slabs, Åhs, M., Sjöberg, A., (2008), Nordic concrete research No. 38, pp 179-192.

Paper V. A quantitative model of moisture redistribution in dual layer concrete slabs with regards to hysteresis, Åhs, M., (2008). Proceedings of the 8^{th} Symposium on Building Physics in the Nordic Countries, Report R-189, Dept. of Civil Engineering, Technical University of Denmark, Kgs. Lyngby, Denmark, pp 873-880.

Paper VI. Influence of early drying of concrete on humidity under impermeable flooring, Åhs, M., Nilsson, L.-O., *(Submitted to Cement and Concrete Research).*

Paper VII. A method to determine the critical moisture level for unsaturated transport of ions, Åhs, M., Nilsson, L.-O., Ben Haha, M., *(Submitted to Cement and Concrete Research).*

Contribution of co-authors

Paper II: Sjöberg contributed in planning the paper, and Anderberg gave detailed instructions on the functionality of the sorption balance.

Paper IV: Sjöberg contributed in planning the paper and assisted in the development of the qualitative model of moisture redistribution.

Paper VI: Nilsson contributed in planning the paper and assisted in the development of the qualitative model of redistribution of moisture after early drying.

Paper VII: Nilsson assisted in developing the moisture conditioning method, Ben Haha developed the method applied to obtain data from the conditioned specimens subjected to the SEM-EDS analysis and performed all SEM-EDS measurements.

Contents

Chapter 1

Introduction

Large quantities of moisture are found in cement based materials in the hardened state, especially in high water cement ratio, w/c, concrete. This moisture is a residue after curing and may cause damage to materials in contact with the concrete. Apart from the adverse impact of the material itself, the damage inflicted by the moisture may also considerably affect the residents' health and well-being. One example where a material may be damaged by this moisture is the adhesive underneath a PVC flooring. In order to avoid this, it is important to assess the moisture distribution in the floor structure, for example before the flooring is applied. By performing this assessment it is possible to estimate the future humidity exposure of the adhesive and the flooring material.

In order to prevent damage caused by the residual moisture the expected maximum humidity level should remain below the critical level. A typical example is concrete floors where this maximum humidity level is achieved just below the flooring when there has been time for the residual moisture inside the slab to be redistributed. A lot would be gained if this expected humidity could be better estimated, for instance on the basis of measurements performed prior to flooring. The critical humidity is often expressed as relative humidity, RH, which is convenient as the RH in a material is a good measure of the expected moisture condition in adjacent materials. In addition, RH measurements on cement based materials are reliable and less affected by uncertainties compared with moisture content measurements [1].

The maximum relative humidity achieved in a homogeneous concrete floor under the flooring may be estimated before the flooring is applied by using the RH method. The RH method includes detailed instructions on how to deter-

mine the RH in a concrete floor slab. Among others, the RH measurement is to be performed at a certain depth to estimate the RH obtained beneath the flooring on homogeneous concrete ground slabs after redistribution. In such slabs the maximum RH level achieved is said to correspond to an RH determined before application of the flooring, at a depth of 0.4h from the slab surface, where h is the thickness of the slab [1].

The Swedish RH method includes detailed instructions on how to report the determined RH together with an estimation of the achieved uncertainty [2]. One of the factors which adds to the uncertainty is temperature fluctuations. Former standards included such fluctuations with an estimated uncertainty. Logged in-situ measurements performed with certified equipment have shown unexpectedly large disturbances as a consequence of temperature fluctuations. This logging equipment, developed to monitor the drying process in concrete floors, is described in detail in Paper I. It has changed the Swedish standards to also include temperature logging.

This thesis presents a method to estimate moisture redistribution in a screeded concrete slab after the flooring is applied. The method considers not only the constituent materials and initial conditions, but also the desorption isotherms and scanning curves. The method is also applicable to homogeneous slabs with consideration taken to scanning.

Additionally, a method is proposed to determine the critical humidity for ion transport in concrete, which is an important factor in promoting adhesive deterioration. This was accomplished by designing an experimental conditioning procedure and by using SEM-EDS to detect alkali redistribution at low concentrations. The conditioning procedure was developed to generate a well-defined moisture state inside a concrete specimen, uniform both in terms of moisture content and relative humidity. This was achieved by utilizing thorough knowledge of moisture fixation and transport and their dependence on moisture history.

A brief theoretical background to cement based materials, moisture and ion transport related properties is presented in chapter 2. Furthermore, the developed qualitative and quantitative models concerning moisture redistribution are described in chapter 3. In addition, a qualitative model of ion redistribution in unsaturated concrete is proposed in that chapter. Input to the models is presented in chapter 4, where moisture properties such as sorption isotherms and examples of repeated scanning curves are shown. In chapter 5, the suggested quantitative model is verified by applying it to a number of screeded concrete slabs. There is a discussion of the presented models and some general conclusions in chapter 6. The last chapter provides suggestions for future research.

Chapter 2

Theoretical background

2.1 Structure of cement based materials

Concrete is made of water, cement and aggregate, and may be treated as a mixture of two separate phases, solid particles and a cement paste, see Figure 2.1. The main purpose of aggregate is to work as a filling material, hence reducing the cement content in the concrete mix. It also serves as a structure for the paste to fix during hardening.

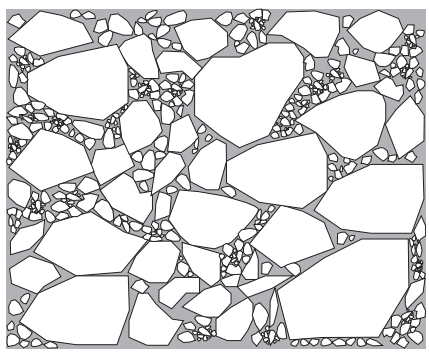

Figure 2.1: Illustration of concrete divided into two phases, white polygons and shaded area representing aggregate and cement paste respectively.

The cement paste is a mix of water and cement. Many different properties of cement paste and hardened concrete are affected by the mass ratio between water and cement, w/c. This ratio quantifies the density of cement grains in the ce-

ment paste, see Figure 2.2. The w/c affects pouring related properties important in fresh concrete, e.g. workability, stability and setting. In the hardened state other properties are affected, such as pore size distribution, porosity, permeability, diffusion coefficients, and moisture content in relation to relative humidity, the sorption isotherm.

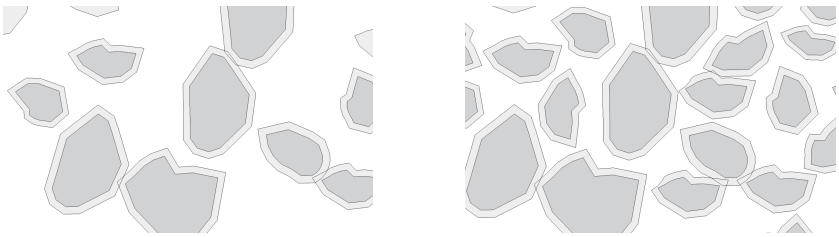

Figure 2.2: Illustration of a high water cement ratio to the left and a low water cement ratio to the right. Water, reaction products (C-S-H gel and others), and cement grains are represented by the white area, lighter and darker shaded polygons respectively.

When cement and water are mixed, chemical reactions are initiated. The reaction that occurs when water becomes chemically bound to the crystal structure of cement is called hydration. At an early stage the hydration rate is high as there are a lot of available unhydrated cement grains surrounded by liquid water. The process slows down when the amount of available water and unhydrated cement decrease.

Reaction products start growing from the surfaces of the cement grains immediately after mixing, see Figure 2.3. As they multiply and grow the reaction products soon bridge the water filled gaps between cement grains and aggregate. The C-S-H gel connects the solid particles forming a complex fine lattice, the concrete hardens.

Figure 2.3: Polygons representing, from left to right, unhydrated, partly hydrated and almost completely hydrated cement grains. The hydration of a cement grain, the C-S-H gel and the unhydrated core are shown as a lighter and darker shaded area respectively.

All pores are believed to be irregular as they are made of building blocks of various shapes; their true shape has not yet been revealed. Many models have been presented throughout history in efforts to explain experimental data, one accepted model is the ink-bottle theory [3, 4]. This theory describes the pores as ink bottles with a narrow neck. Pictures taken with SEM show evidence that pores should be treated more like slit pores [5]. There are a number of more recent models, [6, 7], which were developed in efforts to find a better agreement with new experimental data. Furthermore, a number of models for the nanostructure of C-S-H are summarized by Richardson in [8].

Pores in concrete vary in size from nanometres found in the C-S-H gel, to centimetres, air voids remaining after pouring and compacting. Some of these pores are partly filled with water, some are emptied as the water chemically binds in the lattice and some still remain water filled. Among other things, the pore size distribution determines the concrete's ability to bind water from the surrounding atmosphere, it also influences the moisture transport and capillary suction.

2.2 Moisture fixation in cement based materials

Moisture becomes chemically fixed in the solid because of the cement/water reactions during hydration. Moisture from residual water, exterior liquid sources, and surrounding air becomes physically fixed on material surfaces and in capillary pores by forces originating from molecular attraction, such as cohesion, adhesion, and adsorption.

Moisture in air, which is a mixture of different gases, appears as vapour. The amount of water molecules in air is dependent on environmental conditions. Air above a plane water surface is for example completely saturated, see Figure 2.4, meaning that the maximum water vapour content is reached. The water vapour content is exerting a partial pressure on the air, expressed in Pascal. At atmospheric pressure and temperatures the saturation vapour content is mainly dependent on the temperature.

A practical way of defining the amount of water vapour in air is to relate it to the saturation vapour content, v_s. This relation is often called the relative humidity, RH, and is expressed as a ratio between actual, v, and saturation vapour content in percent RH (% RH).

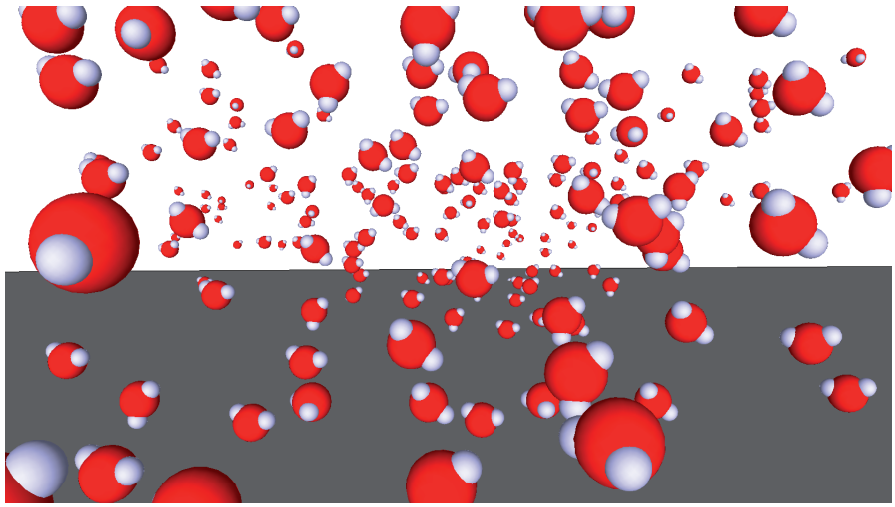

Figure 2.4: Illustration of water molecules in air moving randomly above a flat water surface, shaded area.

A proper definition of the moisture content in air includes both RH and temperature. For example air containing 0.0086 kg/m^3 at 20 °C is equal to a RH of 50 % RH at 20 °C. The RH is calculated using Eq. (2.1).

$$RH = \frac{v}{v_s} \tag{2.1}$$

The vapour content in indoor air is usually limited to about 0.004 - 0.020 kg/m^3. When the saturation vapour content is exceeded the vapour will condense on material surfaces and change to a liquid. The RH level in indoor air regularly fluctuates between some 30 - 70 % RH. Higher RH levels are frequently reached on a short time basis for instance in bathrooms when a resident takes a hot shower. RH below 30 % RH is also reached, for example, in hot indoor premises during winter time when the moisture content of the outdoor air is low.

Physical fixation of moisture vapour on a material surface is linked to the RH in adjacent air. The external and internal surfaces of a dry concrete prism exposed to a humid environment will bind moisture from the air. Water molecules will become attached to it and accumulate on exterior and interior surfaces, see Figure 2.5.

The energy surplus exhibited by the dry material surface will decrease as vapour molecules exhibiting energy deficit attach to the surface. This will hap-

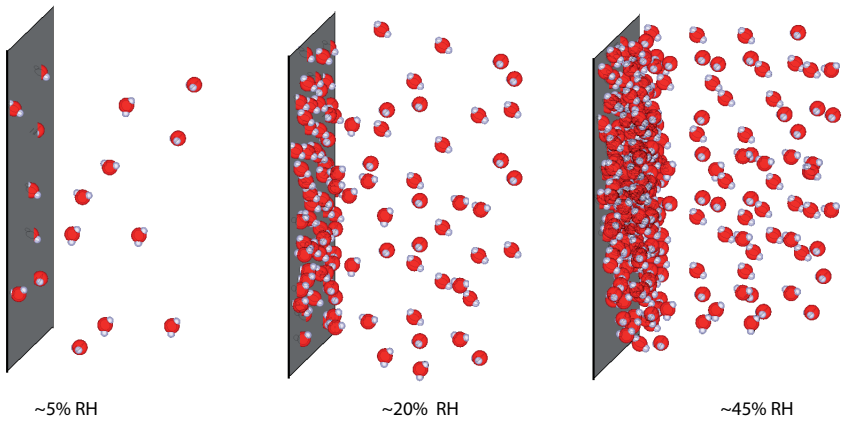

Figure 2.5: Adsorption of water molecules on a material surface, the adsorbate thickness grows from left to right with an increasing RH level.

pen as a result of the chemical potential difference of air borne water molecules and the water molecules attached to a material surface.

Water molecules are merely momentarily attached to the surface on locations called adsorption places. Bonds forming between molecules and surfaces are usually weak hydrogen or van der Waals forces. In contrast to ionic bindings these bindings are easily broken. Molecules continue accumulating on the surface until they reach the lowest possible energy level. This new energy level is called the equilibrium state. At this state an equal amount of molecules attaches to and leaves the surface. As the RH increases, further water molecules stay on the surface for a longer time, ultimately forming a thin water film on the surface.

The process when water molecules are accumulating on a surface is called adsorption and the thin film formed is called an adsorbate, see Figure 2.5. The opposite process is called desorption, when water molecules are released from the surface to the dry air.

Porous materials like concrete exhibit both exterior and interior surfaces available for adsorption, e.g. edges and pore wall surfaces. The pore surface area in ordinary concrete is in the range of 80 - 140 m^2/(g "dry" concrete) [9]. This comparatively large area partly explains the ability of porous materials to adsorb substantial amounts of moisture compared with solid nonporous materials such as metals. Pure adsorption only includes moisture attaching to the surface as a consequence of chemical potential differences.

As the RH increases, further water molecules attach to the adsorbate, ultimately generating a more liquid like film on the surface. There are many theories explaining the nature of adsorption and binding forces between adsorbed molecular layers. One example of monolayer adsorption is the Langmuir theory [10], multilayer adsorption theories include the BET [11] and Dent's gas adsorption theory [12], to mention two of the theories. Dent's equation shows similarities with adsorption isotherms determined for concrete at a relative humidity below some 45 % RH [13]. In Dent's theory water molecules change their properties as they are adsorbed on a surface. Adsorption on a dry material surface is believed to be stronger bound than that on surfaces covered with a film of water molecules. As more molecules become attached the thickness of water film increases, thus gradually decreasing the binding force.

Water surfaces in small pores will curve at the pore walls depending on surface tension forces [14] acting between the adsorbed moisture layers and the material. Suddenly at a certain RH a meniscus is created. This meniscus bridges the empty pore space separating the adsorbed moisture layers, see Figure 2.6.

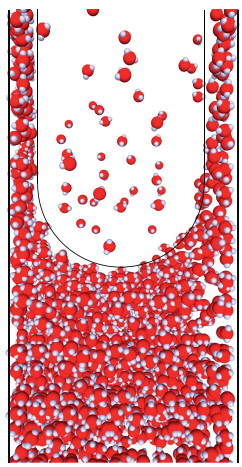

Figure 2.6: Illustration of water molecules moving above a curved water surface in a small pore in concrete.

A hydrophilic material such as concrete will exhibit concave water menisci. The concavity curvature at the pore wall becomes increasingly important as the pore size decreases, the capillary phenomenon exists at pore sizes between 1.4 nm - 0.1 μm. Below 1.4 nm the tensile strength of water is exceeded [13] therefore menisci are considered to be nonexistent below this pore radius.

Saturation pressure above a concave water surface is less than that over a flat surface, and also less over a flat surface than over a convex surface. The Laplace equation [15, 16], was used by Thomson in [17], to derive an expression for the relation between the saturation pressure above a curved surface, p, and the saturation pressure above a plane water surface, p_{sat}. This relation may be rewritten to the familiar expression known as the Kelvin equation Eq. (2.2),

$$\ln\left(\frac{p}{p_{sat}}\right) = -\frac{2 \cdot \gamma \cdot V_m}{T \cdot R \cdot r_m} \tag{2.2}$$

where,γ, is the surface tension, V_m, is the molar volume, T, is the absolute temperature, R, is the gas constant and, r_m, is the mean radius of curvature of the meniscus, also known as the Kelvin radius.

The number of water molecules that exceed the saturation pressure above a concave surface will condense on the meniscus formed by the water, until a new equilibrium is reached, thus enlarging the radius. This process, called capillary condensation, is believed to exist at RH levels exceeding some 45 % RH which corresponds to a Kelvin radius of 1.4 nm in a cylinder shaped pore. Above this level capillary condensation becomes the superior moisture binding mechanism.

The common term used for adsorbed and capillary condensed moisture put together is absorbed moisture. Concrete is able to physically bind substantial amounts of moisture, exceeding 100 kg/m^3.

The external and internal surfaces of a moist concrete exposed to a dry environment release moisture to the air. Completely filled pores at the surface will lose water molecules to the air and menisci will develop. These menisci will break when the saturation pressure above the concave pore radius is less than the actual vapour pressure. However, this breaking of the meniscus corresponds to a lower RH level than that for creating the menisci. All corresponding pores in connection to the surrounding atmosphere at an equal pore size will in due time release moisture to the air.

A sorption isotherm is a property that defines the mass of physically bound water held in a material with respect to RH at a specific temperature. It expresses the equilibrium moisture content in a material in relation to the corresponding RH. The equilibrium moisture content at a certain RH is higher for a saturated cement based material subjected to drying than for a completely dry material moistened to the same RH. The former process, drying of a saturated material sample, is called desorption and the latter absorption. If a process change occurs, for instance from drying to wetting, the RH increases corresponding to a scanning curve.

The desorption and absorption isotherm branches including a scanning curve of a w/c 0.65 concrete determined at 20 °C are shown in Figure 2.7.

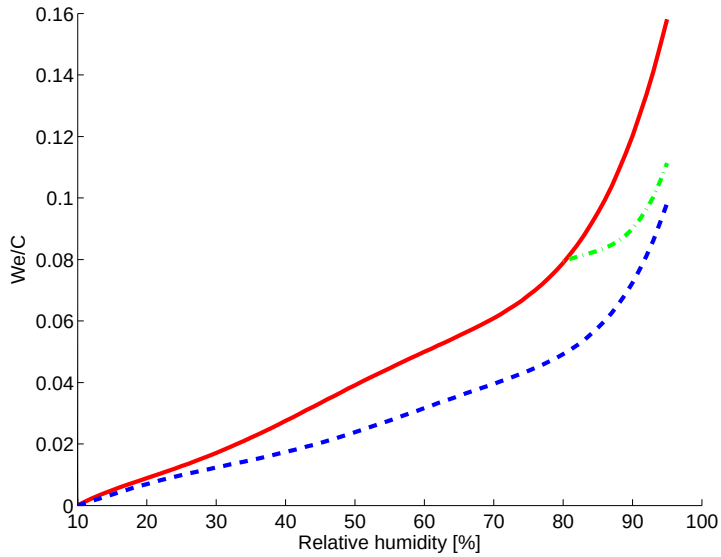

Figure 2.7: Sorption isotherm of a w/c 0.65 concrete between 10 - 95 % RH, including one absorption scanning curve determined from 80 - 95 % RH. The desorption isotherm is represented by the solid line, absorption scanning curve by the dash dotted line, and the absorption isotherm by the dashed line.

Inside this area spanned by the two sorption isotherms every combination of moisture content and RH is obtainable depending on the preceding moisture history. When a material like concrete is re-wetted at some humidity level, after an initial drying, the increase in RH will give rise to a new isotherm, a scanning curve, see dash dotted line in Figure 2.7.

A material showing a desorption isotherm separated from the absorption isotherm is said to exhibit hysteresis. A general definition of the hysteresis phenomenon by Everett [18] states that

> *A process is said to exhibit* hysteresis *if, when the direction of change of an independent variable x is reversed, a dependent variable Y fails to retrace the values through which it passed in the forward process; the dependent variable "lags behind" in its attempt to follow the changes in the independent variable…*

In other words a material is said to exhibit hysteresis if the moisture content in a material during desorption fails to retrace its values while it was absorbing moisture. Cement based materials like concrete exhibit hysteresis to a variable degree.

There are a number of theories of why adsorption hysteresis occurs in a porous material like concrete. The classical ink bottle theory developed from two articles by Kraemer [3] and McBain [4], is one example of a model which may explain the hysteresis phenomenon. The ink bottle theory is based on the assumption that the pores are interconnected with varying sizes of radii and have the shape of ink bottles.

One key requirement for adsorption hysteresis to occur is that there is at least one spontaneous irreversible step change when there is a change from a drying to a wetting mode. This irreversible step could be described to exist in an open ended cylinder where the building of a meniscus does not occur at the same humidity as its collapse, see Figure 2.8 left.

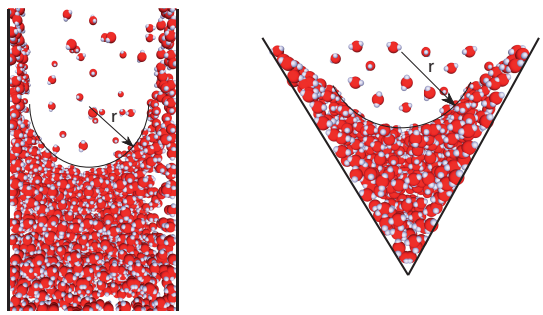

Figure 2.8: Illustration of a concave meniscus formed in a cylindrical (left) and a tapering (right) pore as a consequence of multiple layers of water molecules and capillary condensation, r is equal to the Kelvin radius.

This means that the capillary condensation phenomenon on its own is not enough to achieve hysteresis. In a tapering pore, see Figure 2.8 right, capillary condensation should occur reversibly, as capillary condensation during absorption occurs at the same RH level as it ceases during desorption.

2.3 Moisture transport in cement based materials

There are, traditionally, three basic mechanisms governing moisture flow through a material; capillary suction, diffusion and convection. Moisture flow through

a cement based material like concrete occurs in the cement gel and is governed by capillary suction. Transport of moisture through a gas, i.e. air, by convection originating from an external air pressure difference is insignificant in this study.

Diffusion is defined as transport of matter through a fluid, air or liquid, due to differences in chemical potential, both occurring in cement based materials. The chemical potential may be described as concentration differences occurring from unevenly distributed molecules in a confined fluid volume. The molecules will eventually become uniformly distributed because of diffusion. Such transport is spontaneous and comes from the random motion exhibited by all molecules immersed in a fluid.

The predominant diffusion in concrete takes place as water vapour transfer through air in the communicating pore system. Diffusion of entrained air through water also takes place in partly filled capillaries. Moisture diffusion also exists on a molecular level in the thin layer of adsorbed water molecules on the pore walls. A selection of findings shows that this surface diffusion exists in porous materials like amorphus silica [19], and porous glass [20]. In addition there are findings which have shown minute flow of condensate. In 1952, Carman showed such a flow [21].

The rate of diffusion in concrete is dependent on the porosity, moisture content and tortuosity of the concrete. The diffusion rate increases with porosity and decreases with moisture content and tortuosity.

The total flow is a sum of both vapour flow and capillary flow given by Eq. (2.3),

$$J_{tot} = J_v + J_l \Rightarrow J_{tot} = -\delta_v \frac{\partial v}{\partial x} - \frac{k_p \cdot \partial p_w}{\eta \cdot \partial x} \tag{2.3}$$

where, J_v, represents the vapour diffusion moisture flow and J_l, represents moisture flow due to pressure differences. δ_v, represents the vapour diffusion coefficient, v, represents the vapour content, x, represents the depth from surface, k_p, represents permeability, p_w, represents pore water pressure, η, represents viscosity, and x, represents tube length.

However, up to date it has not been possible to separate these two moisture flows. Diffusion and capillary suction are therefore usually treated as one, and represented by one resistance coefficient, called the diffusion coefficient, see Figure 2.9.

Irregularities of the pore system, see Figure 2.10, are described by the tortuosity factor. The tortuosity factor, τ, indicates the distance a water molecule has to travel to flow through the material, a tortuosity factor of 1 indicating a straight path.

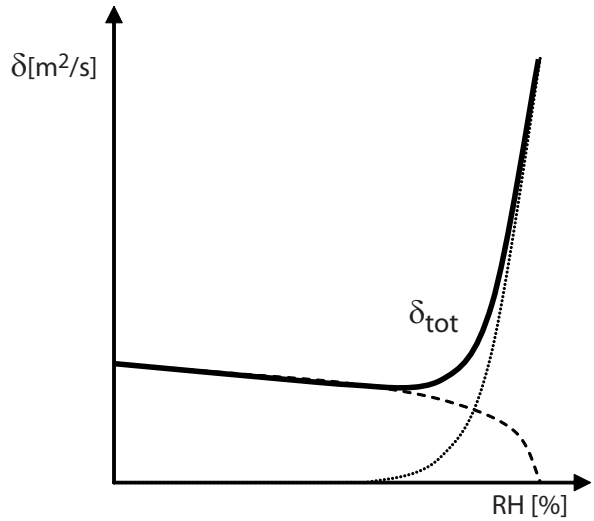

Figure 2.9: Illustration of the diffusion coefficient in relation to relative humidity. The dotted line represents the resistance to moisture flow as capillary suction, the dashed line the resistance to vapour diffusion, and the thick solid line the total diffusion coefficient.

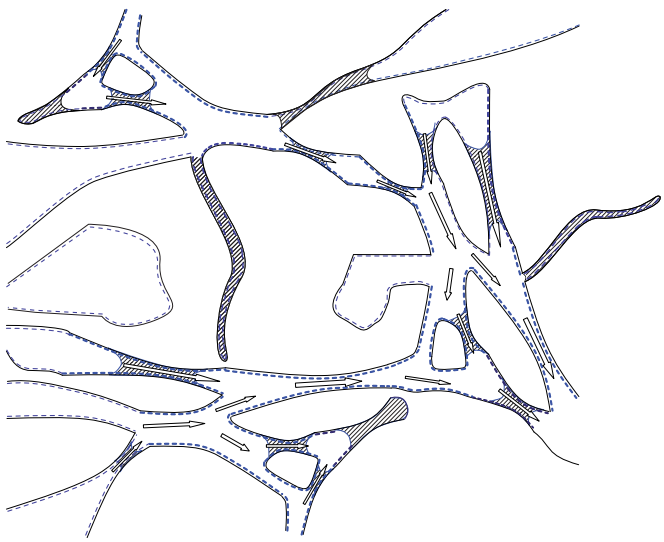

Figure 2.10: Illustration of the tortuosity, some pores are filled with water. Solid lines represent pore walls and dashed lines represent absorbed layers of water molecules. The arrows represent the direction of moisture flow.

2.4 Ion transport in cement based materials

Transport of ions in hardened cement based materials is dependent on moisture in a liquid state. Without water as a solvent, ions are crystallized and therefore unable to move. Ion transport in *saturated* concrete may occur because of concentration differences (diffusion in a liquid) and moisture flow (convection) because of a pressure difference, not necessarily coexisting and not necessarily unidirectional. In *unsaturated* concrete, transport of moisture is caused by moisture flow driven by the pressure difference due to concave menisci, capillary transport, adsorbed water flow and vapour diffusion in the air filled pores. Ions are not conveyed by the vapour diffusion mechanism. It is therefore presumed that the major part of ion transport is governed by the liquid flow, referred to as convective transport, and a minor part by ion diffusion in continuous paths of liquid pore water. The number of published studies describing ion transport in unsaturated concrete is fairly low [22–35].

Various quantities of liquid moisture in unsaturated concrete are found not only as capillary condensed water, but also as thin layers of adsorbed moisture. The quantity is mainly related, apart from temperature, to the RH in the pore system, pore size distribution and whether the present moisture state was obtained by drying or wetting, see section 2.2. This means that there is no fixed relation between the quantity of liquid moisture and RH. The maximum liquid moisture content occurs when the present moisture condition is obtained from a pure drying process. At high moisture content, most of the physically bound moisture is found as capillary condensed water, in contrast to low moisture content where all physically bound moisture exists as adsorbate on pore surfaces.

Ions are carried along with the convective transport in the direction of flow until an air filled pore is encountered. The air filled pore becomes an effective local obstacle to ion transport, as ions are unable to follow vapour diffusion. In such a case it is possible that the pore system offers a path in another direction. The thin liquid water film constituted by the adsorbed moisture may also add to the ion transport, however presumably to a limited extent compared to the convective ion transport by capillary suction. The diffusion mechanism of ions in the adsorbed moisture is disregarded in the following.

As mentioned above there are local obstructions to ion transport in unsaturated concrete. These obstructions occur because of a decrease in moisture content, i.e., the presence of continuous water paths is reduced, see Figure 2.11. This decrease in moisture content reduces the available liquid volume for ions to dissolve into.

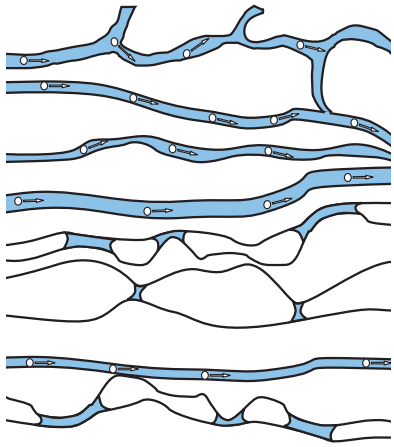

Figure 2.11: Illustration of ion movement in the pore network, some pores are filled with liquid moisture (shaded areas) some are not. Solid lines represent pore walls and pore menisci, and ions are represented by white circles. The arrows indicate the direction of ion movement as a consequence of moisture flow.

Pure desorption

During drying the breaking of the continuous liquid paths occurs first at the concrete surface since moisture interchange with the surroundings takes place there. Hence, it is reasonable to suppose that ion transport to the surface is the first to stop. When the concrete RH at the surface is below the critical RH, ion transport to it completely stops. As capillaries (also in the gel pores) are emptied below the critical RH there are no continuous paths of water reaching the surface. This conclusion is based on the postulate that capillary condensed moisture is removed from the pore system below the critical RH. When drying occurs at a RH level above the critical the quantity of capillary condensed moisture increases. This capillary condensed moisture provides an opportunity for ion movement to the surface.

Scanning

In addition to the breaking of continuous water paths, their growth at re-wetting is an important issue that must be taken into account. The growth does not occur at the RH level at which they are broken, but at a higher level. This means that the humidity increase after an earlier decrease must be considerably higher

than the former until the broken continuous paths are re-established. The opportunity for ion transport has therefore significantly decreased if the concrete has undergone drying before entering the current moisture state. This breaking and re-establishing is furthermore involved when the humidity decreases subsequent to an increase.

Ion accumulation

Ion accumulation may occur in proximity to the drying surface where the moisture content is too low to allow further transport. At a larger distance from the surface, ions are still conveyed towards the dry zone. This would mean that an ion content peak may form with a maximum at a certain distance from the surface [28, 34].

Transport of ions in the hygroscopic range has been reported previously in [23–26, 28–30, 36–38]. These authors suggest a number of different strategies to generate and determine ion transport. One technique is to put ground solid NaCl in contact with conditioned mortar specimens and thereafter determine the chloride ingress [23]. Another technique [24–26] has been to measure chloride ingress after exposure to Cl_2 at different degrees of saturation. Francy [28] used impedance spectrometry to quantify the chloride diffusion coefficient at various RH-levels. Nielsen and Geiker [29] immersed specimens conditioned to a series of RH-levels in a salt solution. Angst [30] mixed various amounts of NaCl into the concrete mixes. Wengholt-Johnsson [36] and Anderberg [37] studied alkali transport from a partly dried concrete to a screed. A completely different approach was applied by Nilsson et al. [38], they detected ion transport by determining the distribution of K_2O in concrete specimens subjected to a number of different drying conditions.

Chapter 3

Models

In this chapter a model of redistribution of residual moisture in homogeneous slabs is presented in the first section. In the second and third sections of this chapter two models are presented, a qualitative and a quantitative model, which may be utilized to comprehend and assess redistribution of residual moisture in screeded slabs. The fourth section presents a qualitative model of moisture redistribution after early drying and the fifth section presents a qualitative model of alkali redistribution.

3.1 Previous model of moisture redistribution

In 1978 a method was developed to determine the future maximum humidity obtained beneath flooring in a drying homogeneous concrete slab [1]. This model is based on the assumption that no moisture leaves the slab after flooring, that the slab base is also sealed, and that isothermal conditions are present. The residual moisture inside a sealed slab will be redistributed until the RH level settles on a uniform vertical level, see Figure 3.1. This method only gives a rough RH estimation as it is based on a computer simulation performed where a homogeneous w/c 0.65 concrete slab is subjected to single sided drying, and the effect of hysteresis is neglected. According to this model a standard depth of 0.4h was decided as an equivalent depth where the humidity level is equal to the maximum RH later achieved beneath the flooring. This relation between RH before and after flooring is based on a computer simulation performed in the late 1970s, where a homogeneous 100 mm concrete slab is drying from one side at 20 °C

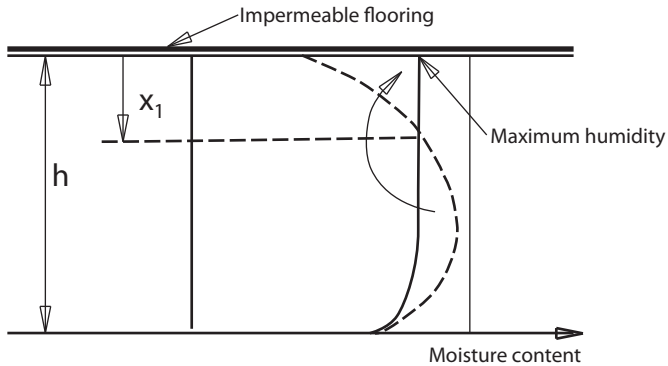

Figure 3.1: The depth x_1 at which the RH level prior to flooring corresponds to the maximum RH level that occurs after flooring installation [1].

and 40 % RH, [1]. Depending on the simulated drying time before flooring the depth from the surface varied between 0.35 and 0.42 of the slab thickness. The simulations are based on the simplification that the RH and moisture content may be described in one single equation. The relationship between RH and moisture content, sorption isotherm, is far more complex.

A sorption isotherm for a single concrete mixture was used in the simulation, without considering hysteresis. This omission of the hysteresis may have an impact on the estimated RH obtained from the simulation.

The method is not applicable to screeded floors. A new method is therefore needed in order to estimate the maximum humidity in such floors, a common construction today. This method is also applicable to homogeneous floor slab constructions and is an improvement to the current model. In the next section moisture redistribution is described qualitatively. In section 3.3 a proposed quantitative model is described.

3.2 Qualitative model of moisture redistribution

In this section a qualitative model is presented which describes the RH distribution for a two material combination, e.g. a screeded concrete slab. Three distinctive phases, drying of the slab, screed application and drying, and redistribution in the screeded slab after flooring, illustrate important stages from a moisture distribution perspective in the production of a screeded floor. These phases are presented together with a corresponding sorption isotherm and scanning curves in Figure 3.2.

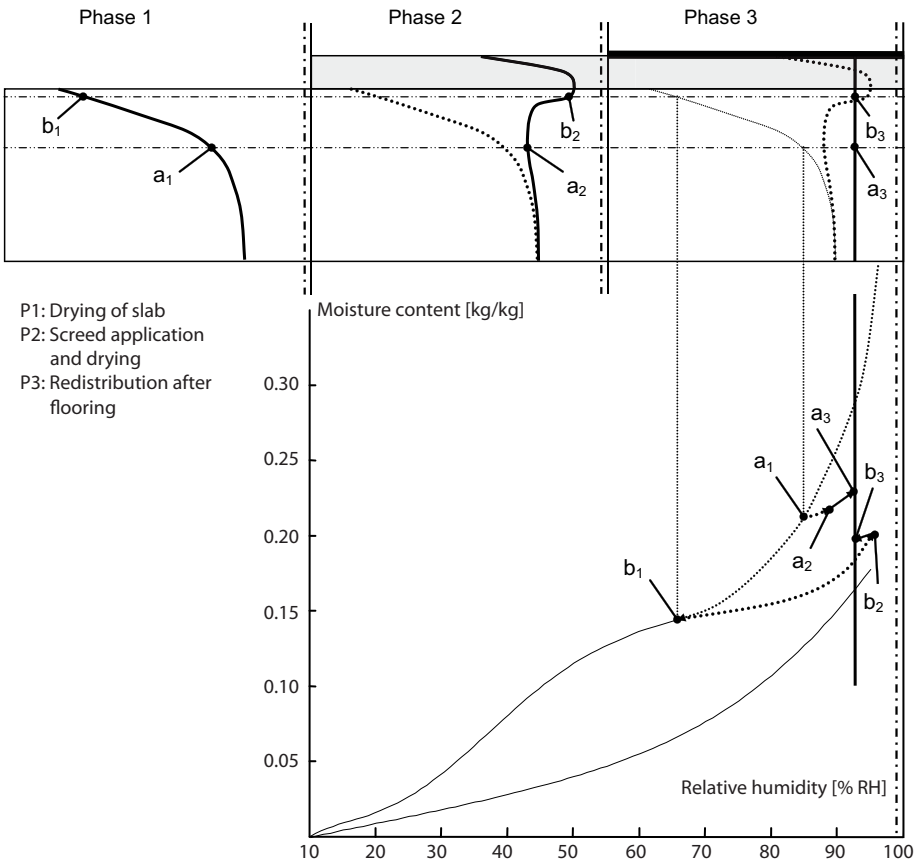

Figure 3.2: Phase 1 shows the distribution of residual moisture (as RH) in a concrete slab after some drying. A wet screed is applied in phase 2 and subjected to drying, and finally moisture is redistributed after flooring. Underneath a typical sorption isotherm is shown where a_i and b_i, indicate two material sections and the subscript indicates the corresponding phase number.

The slab represents a homogeneous slab sealed at the base which is drying upwards. Thick dotted lines show the initial moisture distribution in each phase and solid thick lines represent the moisture distribution just before the next phase is entered. The moisture distribution in phase 1 is included as a thin dotted line in phase 3 to facilitate comprehension of the overall moisture redistribution changes and corresponding changes in the sorption isotherm. These changes are indicated for two slab sections, a_{1-3} and b_{1-3}, which are particularly interesting from a moisture redistribution perspective.

In the first phase a concrete slab drying from one side only is shown. The moisture distribution clearly demonstrates a high humidity at the slab base and a lower humidity at the surface. A wet screed is applied on the semi-dry concrete slab in the second phase. This wet screed dries from the top surface and simultaneously moisture penetrates downwards into top surface of the slab. Later, some of the moisture is redistributed towards the slab base. In addition the screed top dries as shown before the second phase is finished. Finally, the third phase shows the moisture distribution when phase 2 is left and after flooring when internal moisture redistribution is completed.

In Figure 3.2 letters (a) and (b) represent material sections where the moisture content follows a particular path in the typical sorption isotherm diagram displayed in the same figure. Letter (a) corresponds to a section somewhat above the slab centre. In the first phase the moisture content decreases, following the desorption isotherm down to point a_1. Subsequently, after screed application, this section's moisture content increases, following an absorption scanning curve up to point a_2 and finishes at point a_3. Letter (b) illustrates a material section somewhat below the top surface of the slab where the moisture content decreases to point b_1, following the desorption isotherm. In phase 2 the moisture content increases by following an absorption scanning curve up to point b_2 and finally decreases finishing at point b_3 by following a desorption scanning curve.

3.3 Quantitative model of moisture redistribution

A theoretical model is proposed that suggests how the future moisture distribution in a screeded slab, which occurs after flooring is applied, can be estimated. The following simplifications are made:

- no further drying of the slab will occur; residual moisture will be redistributed
- isothermal conditions
- moisture transport is not quantified
- homogeneous materials

When a screeded slab is sealed the residual moisture will be redistributed, ultimately attaining a uniform vertical RH distribution, see the red line in Figure 3.3.

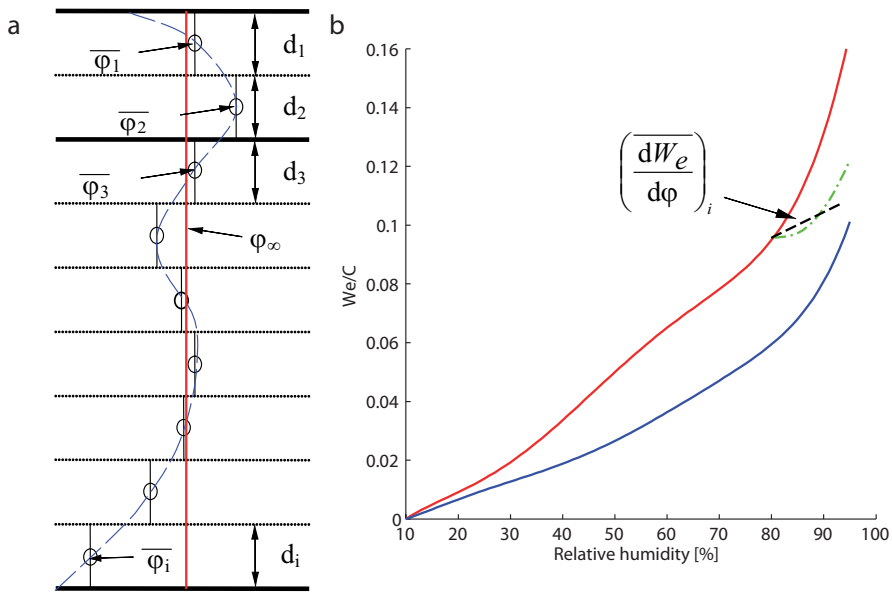

Figure 3.3: Illustration (a) shows the RH distribution in a screeded slab before flooring is applied (dashed line). The solid red line illustrates a possible uniform RH distribution after sealing. Illustration (b) shows a typical sorption isotherm including one scanning curve (dash dotted line) and the average moisture capacity (dashed black line) for this scanning curve.

The change in moisture content in each section is given, provided that each section's moisture history, RH change, and "moisture capacity" are known. The moisture capacity, ξ, for a certain RH is defined by Eq. (3.1),

$$\xi = \frac{dW_e}{d\varphi} \tag{3.1}$$

where, dW_e, represents the difference in evaporable water in kg/m^3, $d\varphi$ represents the difference in relative humidity in % RH, see the dashed line in Figure 3.3.

This property shows how much a moisture content change is affected by a change in RH. Figure 3.4 shows that a change in RH from 80 - 85 % RH does not change the moisture capacity as much as a change from 85 - 90 % RH does. In other words a steep sloping isotherm gives rise to a high moisture capacity and a gentle sloping isotherm gives rise to a low moisture capacity. This means that

small moisture transfers from wet to dry regions in a concrete change the RH level according to the previous history of the moisture receiving region.

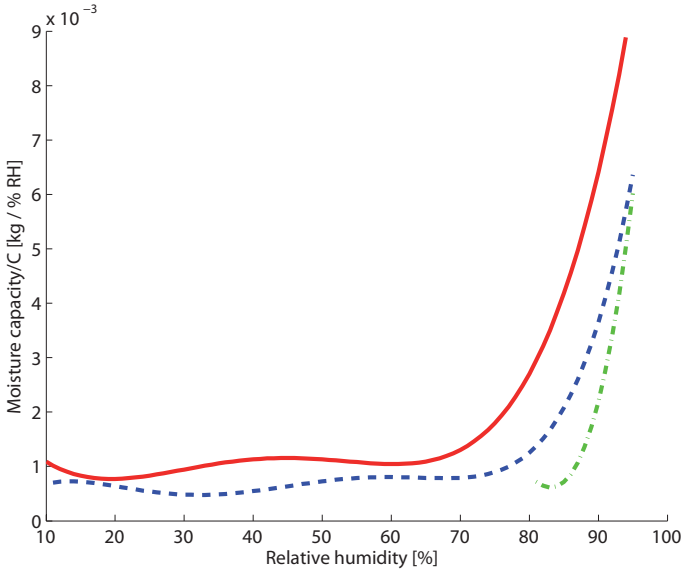

Figure 3.4: Illustration of the moisture capacity of a w/c 0.65 concrete including the moisture capacity of a scanning curve determined in the 80 - 95 % RH range. The moisture capacity of the desorption isotherm is represented by the solid line, the absorption scanning curve by the dash dotted line, and the absorption isotherm by the dashed line.

As the total moisture content will be maintained in the sealed slab it is possible to calculate the uniform RH level. This is done by adding the change in moisture content in all sections. As no moisture is lost this sum must be zero. The solution to this problem is obtained by iteration.

Based on the assumption that no moisture will escape from the screeded slab, the uniform RH level will settle somewhere in between the extremes of the RH distribution prior to sealing. A reasonable initial guess may be the mean RH. The next step will be to determine the moisture history of each section in order to assign a realistic moisture capacity.

Judging from Figure 3.3 both the slab base and screed sections have only experienced drying prior to flooring. Therefore they must be assumed to have reached their moisture content and corresponding RH level by following the desorption isotherm. Top slab sections, on the other hand, have experienced both drying and wetting prior to flooring, thus obtaining their moisture content

and RH level by following a scanning curve. The above qualitative analysis is of great importance when the future redistribution of moisture is determined.

The future moisture content in each section is determined from the preceding drying-wetting history as well as the expected moisture gains or losses to adjacent sections in the future. If a section following a desorption isotherm will lose moisture to attain the guessed RH level, its moisture capacity will be determined from the desorption isotherm. If, on the other hand, a section follows the desorption isotherm and suddenly starts to gain moisture, the moisture capacity is obtained from a scanning curve. And finally, sections already following an absorption scanning curve will either continue to follow the absorption scanning curve or, if losing moisture, follow a scanning desorption isotherm.

The assumption of no further drying implies that the moisture content per square metre of the screeded slab is constant before and after the flooring.

The above reasoning and simplifications could represented by an arithmetic expression Eq. (3.2),

$$\sum_{\Delta x_i} (\overline{\varphi_i} - \varphi_\infty) \cdot d_i \cdot \left(\overline{\frac{dW_e}{d\varphi}} \right)_i = 0 \tag{3.2}$$

where $\overline{\varphi_i}$, expressed in [% RH], represents the RH determined in section d_i, φ_∞, expressed in [% RH], represents the uniform moisture distribution obtained after a redistribution is finished, d_i represents the thickness of the section expressed in [m], $\left(\overline{\frac{dW_e}{d\varphi}} \right)_i$ expressed in [kg/m^3]represents the average moisture capacity of section d_i obtained from the sorption (scanning) isotherm at the current RH.

By rearranging Eq. (3.2), Eq. (3.3) is obtained.

$$\sum_{\Delta x_i} \overline{\varphi_i} \cdot d_i \cdot \left(\overline{\frac{dW_e}{d\varphi}} \right)_i - \sum_{\Delta x_i} \varphi_\infty \cdot d_i \cdot \left(\overline{\frac{dW_e}{d\varphi}} \right)_i = 0 \tag{3.3}$$

Equation (3.3) shows the change in moisture content with respect to each section's change from $\overline{\varphi_i}$ to φ_∞. As the slab is assumed sealed no moisture is lost, thus the sum the moisture content changes in all sections is 0 (zero). Equation (3.3) may be rewritten as

$$\sum_{\Delta x_i} \overline{\varphi_i} \cdot d_i \cdot \left(\overline{\frac{dW_e}{d\varphi}} \right)_i = \sum_{\Delta x_i} \varphi_\infty \cdot d_i \cdot \left(\overline{\frac{dW_e}{d\varphi}} \right)_i \tag{3.4}$$

As the final uniform RH, φ_∞, is constant throughout the slab it may be moved outside the summation mark.

$$\sum_{\Delta x_i} \overline{\varphi_i} \cdot d_i \cdot \left(\overline{\frac{dW_e}{d\varphi}}\right)_i = \varphi_\infty \sum_{\Delta x_i} d_i \cdot \left(\overline{\frac{dW_e}{d\varphi}}\right)_i \tag{3.5}$$

Finally the sum on the left side of Eq. (3.5) is divided by the sum of the section thickness multiplied by moisture capacity leaving the uniform RH, φ_∞, on the right side resulting in Eq. (3.6).

$$\varphi_\infty = \frac{\sum_{\Delta x_i} \overline{\varphi_i} \cdot d_i \cdot \left(\overline{\frac{dW_e}{d\varphi}}\right)_i}{\sum_{\Delta x_i} d_i \cdot \left(\overline{\frac{dW_e}{d\varphi}}\right)_i} \tag{3.6}$$

The resulting φ_∞ is thereafter compared with the initial guess. If the difference is large then a new calculation needs to be performed by replacing the initially guessed φ_∞ with the resulting φ_∞. The moisture capacity for each section changes accordingly. This model is verified in chapter 5.

3.4 Qualitative model of redistribution of moisture after early drying

The purpose of this section is to suggest a qualitative model that considers aspects of hydration in a homogeneous floor structure with respect to redistributed moisture during drying. It is assumed that some of the redistributed moisture becomes a part of the solid matter and thereby reduces the increase in humidity below a semi-permeable flooring.

The model assumes a drying environment below 80 % RH before a non-permeable flooring is applied on the floor structure. This is to achieve a substantial humidity decrease at the concrete surface facing the dry environment. Exposure to a dry environment reduces the rate of cement hydration [39, 40], and these dry conditions are mainly achieved in shallow parts of a floor structure. The reduction in degree of hydration may have an impact on the humidity below the adhesive in a floor structure after flooring. The less hydrated cement grains may react with the redistributed moisture and therefore bind some of it chemically. This additional hydration may lower the anticipated RH at the surface, by a delayed self-desiccation, hence reducing or even preventing a moisture damage, i.e. adhesive deterioration.

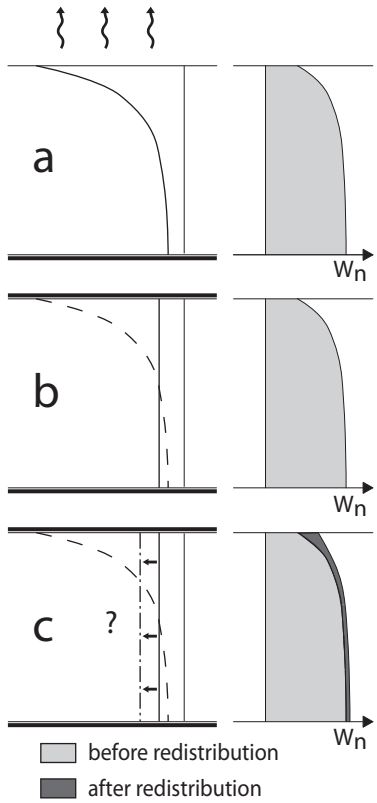

Figure 3.5: a) Single sided drying of a concrete floor slab b) Redistribution of moisture under an impermeable flooring without considering additional chemical binding c) Redistribution of moisture and chemical binding of redistributed moisture.

The suggested mechanism behind the decrease in humidity caused by a continuing hydration is illustrated in Figure 3.5.

The left figures (a-c) show the moisture distribution, MD, and the right figures show the distribution of degree of hydration, represented by w_n. The solid line in (a) represents the MD before redistribution, and in (b) and (c) they represent the MD after redistribution. The dashed lines in (b) and (c) represent the MD before redistribution and the dash dotted line in (c) represents the expected humidity after redistribution. The figures represent from top to bottom

a) The original moisture distribution before redistribution in a floor slab dried from one side only.

b) The floor slab after moisture redistribution where no additional hydration has occurred.

c) The floor slab after moisture redistribution where additional hydration has occurred, especially in the top part with most drying, and the level of humidity has decreased compared with Figure 3.5b.

3.5 Qualitative model of ion redistribution during drying

The aim of this section is to propose a simple qualitative model of ion redistribution in a homogeneous concrete slab subjected to drying. The following assumptions are made:

- Ion transport occurs only at a RH above a certain critical level.
- Ion transport will be larger at a higher RH-level.

Redistribution of ions, in this case, is initiated by a dry environment surrounding the moist concrete structure. This surrounding environment generates a moisture flow, which may convey ions to the drying surface. As mentioned in section 2.4, ions are only able to migrate in liquid moisture in the capillaries. Therefore, ion transport decreases with the emptying of the capillaries.

When drying occurs at a RH below a critical RH level, capillaries in the concrete structure become air filled when equilibrium is attained. Until the surface material reaches a humidity below the critical RH level, some capillaries are still able to convey ions to it. The ions are consequently gradually prevented, because of the air filled capillaries, from reaching the surface. Because of these obstacles, ion accumulation occurs at a small distance from the surface, where enough capillaries are still filled with liquid moisture. This accumulation process continues until the humidity drops below the critical RH level further into the material. This kind of drying process may create a peak of ions located next to the surface, see Figure 3.6 left.

Drying may also occur at a higher humidity level, at which moisture filled capillaries reach the surface during drying and still do at equilibrium until moisture transport ends. The ions are therefore conveyed to and accumulated at the surface, see Figure 3.6 right. The accumulation at the surface in this case does not stop until equilibrium with the surrounding humidity is attained. The peak at the surface gives rise to an uneven distribution which generates a potential for

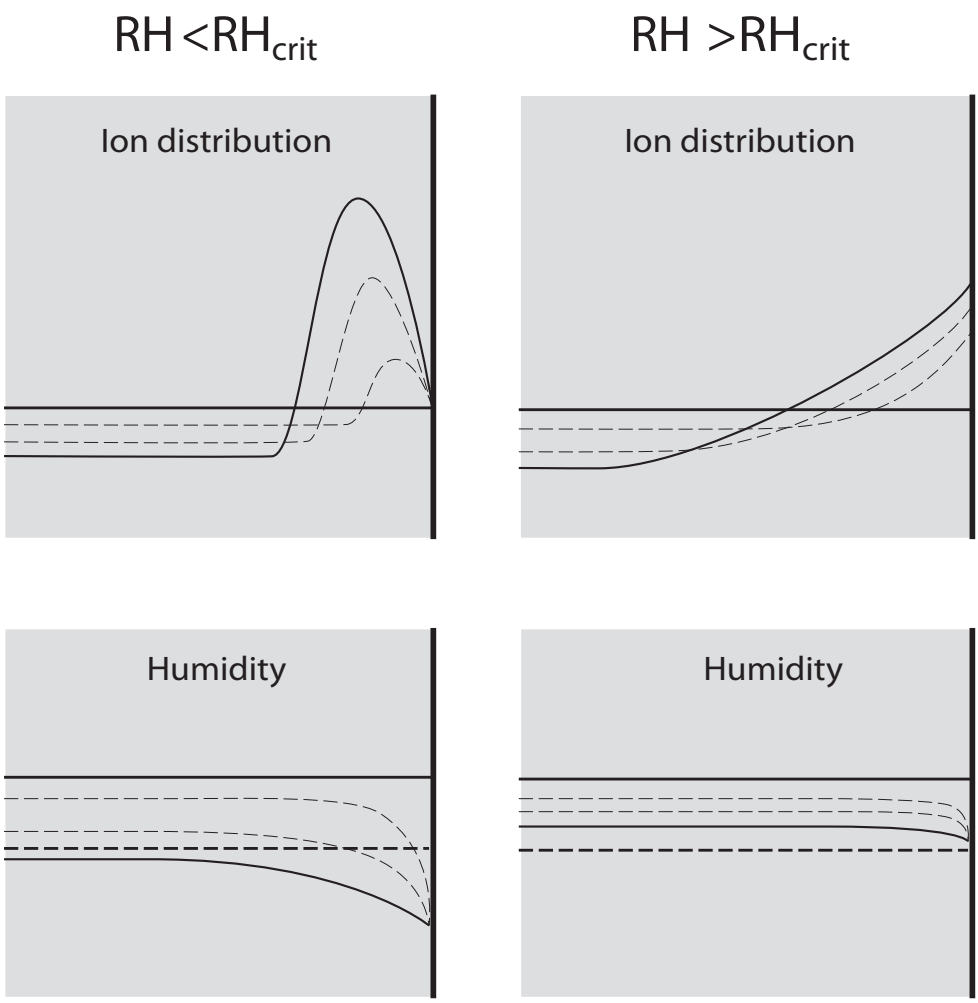

Figure 3.6: Redistribution of ions during drying at a surrounding humidity below (left) and above (right) the critical humidity (thick dashed line).

a diffusion process transporting ions in the opposite direction to moisture flow. This diffusion transport is not hindered as effectively as if the drying climate were lower than the critical humidity.

Both of these drying actions may be combined into one qualitative model of ion redistribution during drying, see Figure 3.7. This model is based on the material's pore system and an assumption that the system to some extent consists of inter-connected pores in which continuous liquid paths are present above a certain humidity, see Figure 3.7a. The humidity at which these paths occur and

are able to convey ions is defined as the critical humidity, RH_{crit}. Furthermore, the pore system in cement based materials is characterized by a wide range of pore sizes. The pore size distribution is decisive for the quantity of liquid moisture at a certain moisture level, and an increase in the moisture level corresponds to an increase in liquid moisture. It is therefore reasonable to assume that there is an increase in ion movement when the humidity increases, see Figure 3.7b.

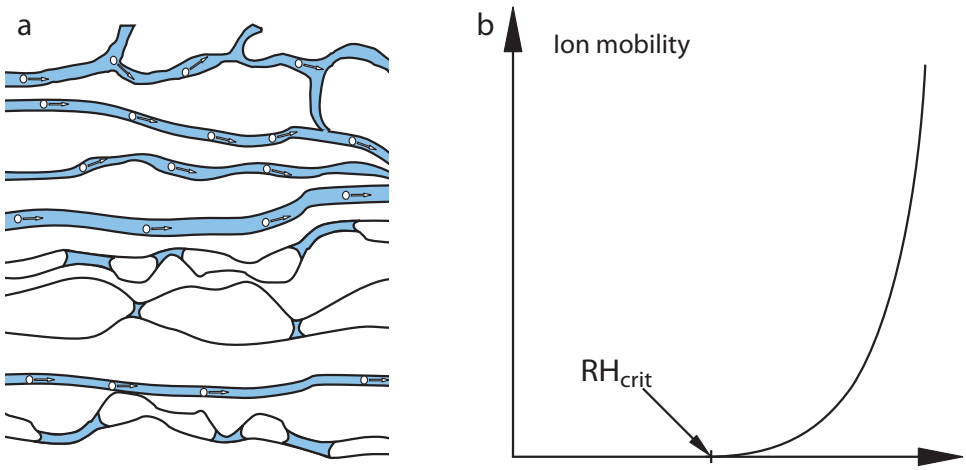

Figure 3.7: Qualitative model of ion redistribution during drying.

Chapter 4

Experimental work

The experimental work in this thesis is presented in this chapter. The manufacture of a number of screeded floor slabs and different materials used in this work is presented in section 4.1. The sorption measurement, applied to determine sorption isotherms of the materials used in the screeded floor slabs, is described in section 4.2 including results. Two methods to determine both absorption and consecutive desorption scanning curves, a comparison between the two and the results obtained are presented in section 4.3. The determined moisture transport properties for some of the materials used are presented in section 4.4, besides the evaluation method. A description of experimental work to investigate the possible beneficial effects of applying drying at an early stage is presented in section 4.5. Finally, the work performed to determine redistribution of alkali in partially saturated concrete is introduced in section 4.6.

4.1 Moisture redistribution

The conducted experimental work followed two basic courses. First of all, test specimens in three batches were manufactured with the aim to replicate the essential characteristics of three common screeded concrete floor constructions. Secondly the material properties were investigated on samples continuously extracted from the floor constructions in order to detect possible property transformations.

Batch 1 was intended to replicate a homogeneous ground slab, Batch 2, an intermediate floor structure, and finally Batch 3, a hollow core slab, HCS. These

batches were produced in full scale regarding thickness, covering an area of 0.5 - 1 m^2, see Figure 4.1.

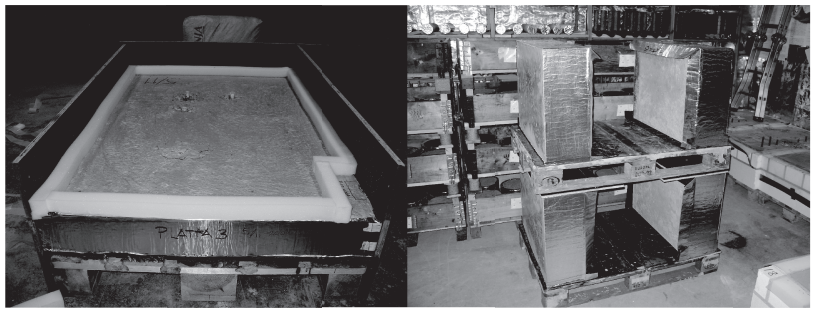

Figure 4.1: Left picture shows one floor construction in Batch 1 prepared for screed application, one corner was spared for sample extraction from the slab. Right picture shows four floor constructions from Batch 2, vertically tilted in a climate conditioned room and not yet covered with screed.

In total, nine concrete floor slabs were produced in this research. Eight homogeneous slabs were manufactured at the laboratory and one HCS was delivered from a factory. The homogeneous slabs were prepared to reproduce two different screed application scenarios, application on a slab subjected to a short period of drying and application on a slab subjected to a longer period of drying. The HCS was prepared to reproduce a situation where a centre hollow core was filled with concrete at the slab end prior to screed and flooring application.

Four cement based materials were used to manufacture the screeded slabs, see Table 4.1. The homogeneous structural slabs were manufactured by using a w/c 0.65 concrete, C. The cement mortar has a w/c 0.55, M, and Floor 4310 Fibre Flow, SFC were used for screed application. Both the concrete and mortar were mixed and poured at the laboratory. The self-levelling flooring compound was delivered as a dry powder mix from the factory. Water was added to the dry powder and mixed in the laboratory according to instructions from the manufacturer. Finally, the HCS was manufactured in a factory by using a w/c 0.4 concrete, C_{HCS}.

Table 4.1: Mixture for each used material. Quantities are presented in kg/m^3.

Material	C	M	C_{HCS}	SFC[1]
Portland Cement CEM II/A-LL 42.5 R	250	400		
Portland Cement CEM I 52.5 R			390	
Portland Cement				1-5
Aluminous Cement				5-20
Gypsum				2-10
Water	162	220	147	20
Dolomite 0.002-0.1 mm				31
Sand 0.1-1 mm				47
Sand 0-8 mm	967	1672	973	
Sand 6-13 mm			851	
Sand 8-12 mm	489			
Gravel 8-16 mm	489			
Polymer				1-5
P30			1.2	
Glenium 51	1.5	2.9		

[1]Mixture according to manufacturer mass-% of dry powder, density 1900kg/m^3

All slabs were subjected to certain drying times in suitable climate rooms before and after screed application. Then a PVC flooring, 2 mm Tarkett Eminent, was installed on all nine slabs by using a water based floor adhesive, CascoProff Solid. Material combinations and application sequences are described in detail in Table 4.2.

Table 4.2: Slab material combination, application sequence, and drying plan.

Batch No.	1				2				3
Slab	1	2	3	4	5	6	7	8	9
Material	C	C	C	C	C	C	C	C	C
1st Drying [days]	105	105	110	110	9	11	408	408	28[2]
Screed	SFC	SFC	M	M	M	SFC	M	SFC	SFC
2nd Drying [days]	48	96	98	90	261	259	40	40	138
Adhesive [m^2/l]	3.6	3.6	3.5	4.3	3.1	3.0	3.3	3.0	3.0
Flooring	PVC	PVC	PVC	PVC	PVC	PVC	PVC	PVC	PVC
Redistr.1[days]	206	158	149	157	269	269	91	91	273
Redistr.2[days]					702	702	729	729	

[2]Initial drying time of the C filling of the mid core, the HCS is cast approx. 60 days earlier.

The humidity distribution was determined in each slab prior to floor application on samples obtained by using a core drill, see Figure 4.2. Subsequent to

floor installation the slabs were put back into the climate room. The moisture distribution was determined once more after a certain time of moisture redistribution, see Table 4.2, and in slabs 5-8 the moisture distribution was determined once again after more than two years after flooring. These moisture distributions are shown in chapter 5. A detailed description of slab preparation, material application and climate conditions is found in Paper IV.

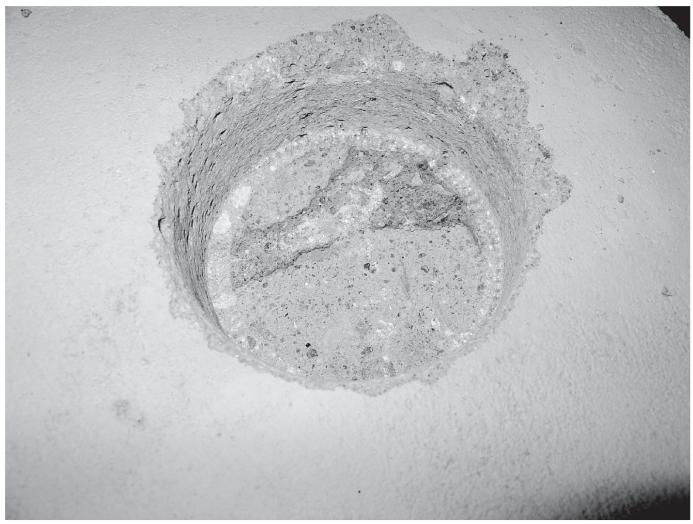

Figure 4.2: The remaining hole from a core drill, 90 mm in diameter, after extracting samples for moisture distribution determination before flooring. Drilling was performed from the top in a homogeneous slab from Batch 1. Note the clear breaking zone separating the mortar screed from the concrete material.

4.2 Sorption measurements

Several sorption measurements were performed on a number of small material samples, 20 - 100 mg, which were obtained from the floor constructions. All but two material samples were chiselled out from the top surface of the material at a depth of about 20 - 25 mm. The two other samples were taken from a depth of 200 mm, in one of the concrete slabs. To avoid carbonated material 10 - 15 mm of the surface material was discarded before sampling. The samples were mainly removed from material subjected to a certain drying time in a 60 % RH at a temperature of 20 °C. Details of the sorption isotherm evaluation are presented in Paper III together with results.

A gravimetric vapour sorption balance, DVS, was used for all sorption isotherm determinations. Its key component is a balance, Cahn D-200, that continuously determines the mass of a sample subjected to a sequence of well-defined constant or variable RH levels. These RH levels are generated from a mixture of dry and saturated nitrogen gas. The generated humid gas stream is split in two before one half passes the reference and the other passes the sample pan. In order to achieve stable conditions the balance is installed inside a climate controlled cabinet. For a detailed description of the sorption balance see Paper II.

Desorption, absorption and scanning curves were determined by changing the RH in the sorption balance stepwise in a certain sequence. The measurements always started with a saturated specimen, which had earlier been subjected to drying. Therefore, the desorption isotherms represent the 2^{nd} desorption. Typical RH sequences are shown in Figures 4.3 and 4.4. The difference between the two sequences is the way RH changes during scanning, with drying followed by wetting or wetting followed by drying. In Figure 4.3 RH changes gradually with time. In Figure 4.4 the change is stepwise.

Each sample was put on a saturated piece of cloth inside a sealed glass container for a minimum period of 24 hours prior to the test, in order to become capillary saturated. Subsequently it was loaded into the sorption balance and subjected to the test sequence.

In order to obtain the asymptotic mass corresponding to each RH level each step change was evaluated by curve fitting according to Eq. (4.1) [41],

$$m(t) = m_f - (m_f - m_0)e^{-k(t-t_0)} \tag{4.1}$$

where $m(t)$ represents the sample mass at the time t, m_0 is the initial mass for each curve fitting, m_f represents the asymptotic final mass, k is a curve fitting constant and t_0 is the initial time for each curve fitting. An illustration of the result from using Eq. (4.1) is shown in Figure 4.5. The best fitting curve was

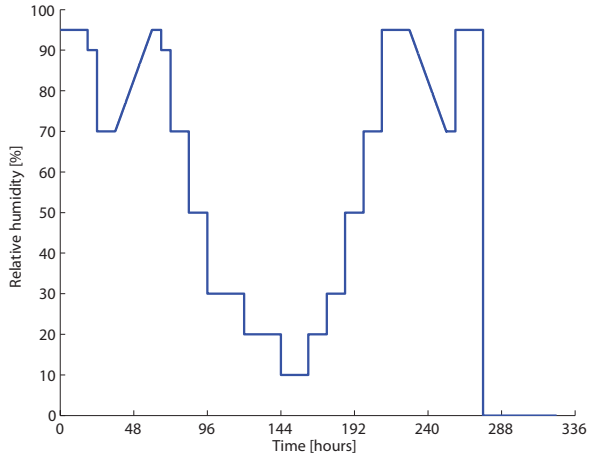

Figure 4.3: Illustration of a typical RH test sequence used in Paper III, where an absorption and desorption scanning curve is determined by using a linearly increasing and decreasing RH.

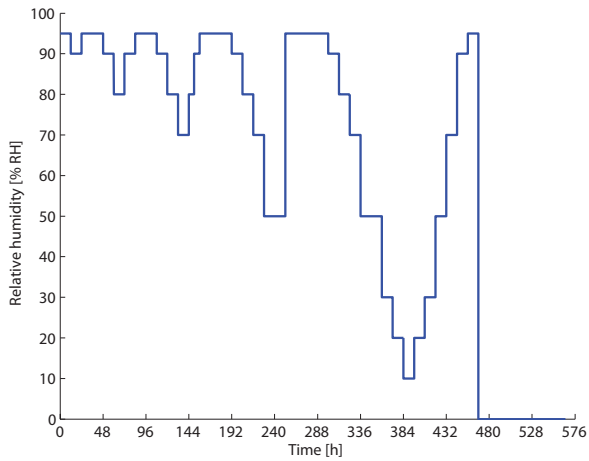

Figure 4.4: Illustration showing a typical test sequence for determining the boundary sorption isotherm loop including inner scanning curve loops by using the most recent method, where RH step changes are used, instead of linearly increasing/decreasing RH.

obtained by the least squares method. This curve fitting is further explained in Paper III. Note that the sample was subjected to 0 % RH at the final step of each test sequence, see Figures 4.3 and 4.4. This arrangement of the 0 % RH exposure was decided on the basis of the hypothesis that chemically bound moisture may be released at RH levels below 10 % RH, thus possibly destroying the material structure [42]. The dry mass was therefore obtained from the curve fitted asymptotic mass at 10 % RH.

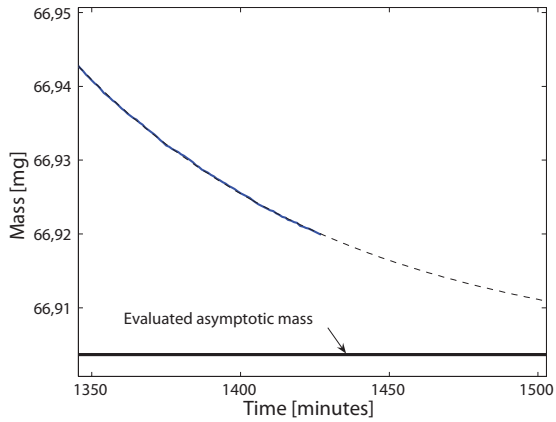

Figure 4.5: Curve fitting of the recorded mass in an RH step to determine the asymptotic final mass for each RH step.

Sorption isotherms were determined for four different materials, two concretes, C and C_{HCS}, cement mortar M, and one flooring compound, SFC. The moisture content is quantified as the evaporable moisture content, W_e, divided by cement content, C, for materials C, C_{HCS}, and M. The cement content was estimated by first quantifying the Ca content in each C, M, and C_{HCS} sample. This was accomplished by using inductively coupled plasma atom emission spectroscopy, ICP-AES. A detailed description of the applied method and the results obtained is found in Paper III. For material SFC the moisture content per mass of material is represented as a fraction of mass at 10 % RH.

Desorption and absorption isotherms for the four materials are shown in Figures 4.6 - 4.9. Additional isotherms determined for C, M, and SFC are found in Paper III. The isotherms determined for material C on samples removed 20 mm from the slab top deviated significantly from isotherms determined on samples removed 20 mm above the slab base. The other materials showed a smaller deviation.

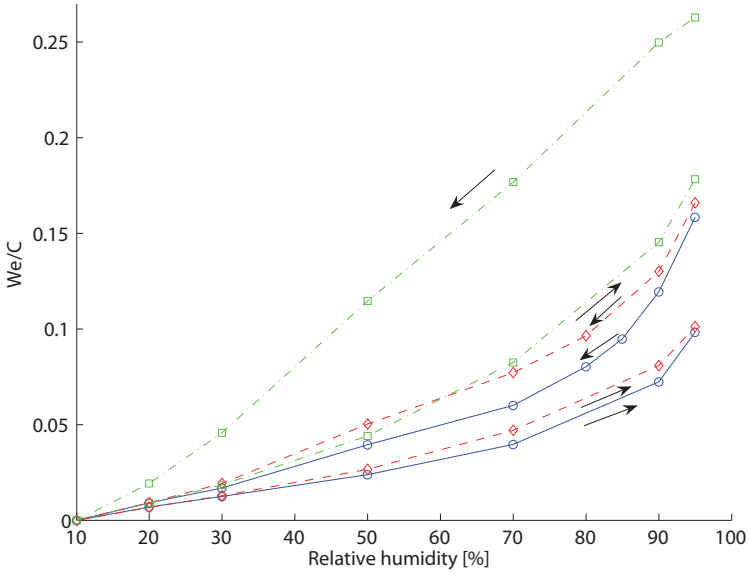

Figure 4.6: Sorption isotherms determined for three samples of material C. One sample, 16 months old (dash dotted line), extracted about 20 mm from the surface facing air, and two samples 9 (dashed) and 12 (solid) months old, extracted about 20 mm from the base surface.

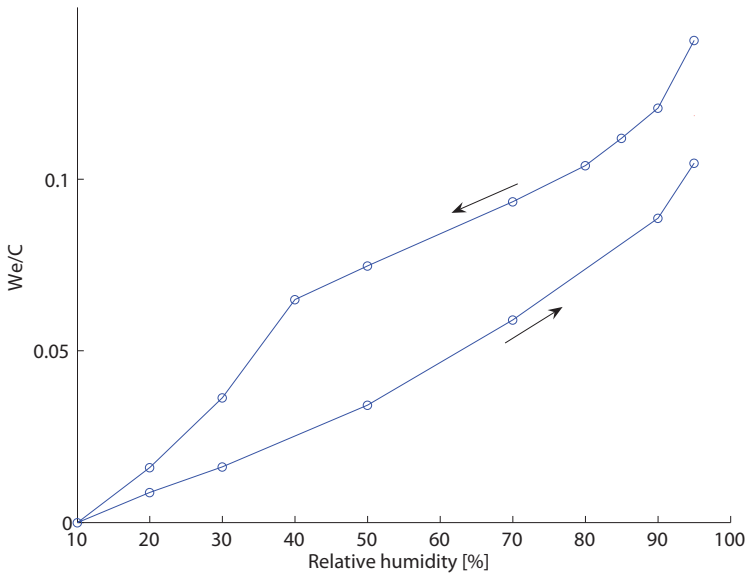

Figure 4.7: Sorption isotherm determined for one sample of material C_{HCS}.

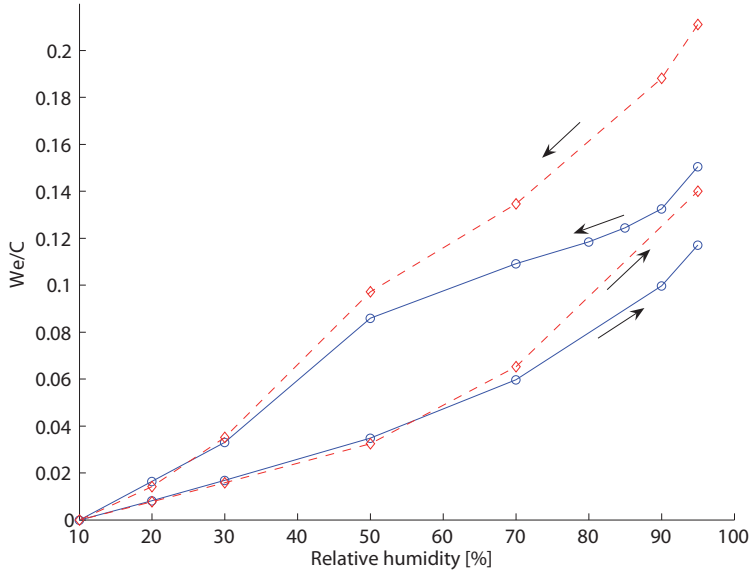

Figure 4.8: Sorption isotherms determined for two samples of material M, w/c 0.55 cement mortar. The dashed line represents a sample subjected to drying for 1 month and the solid line 12 months of drying.

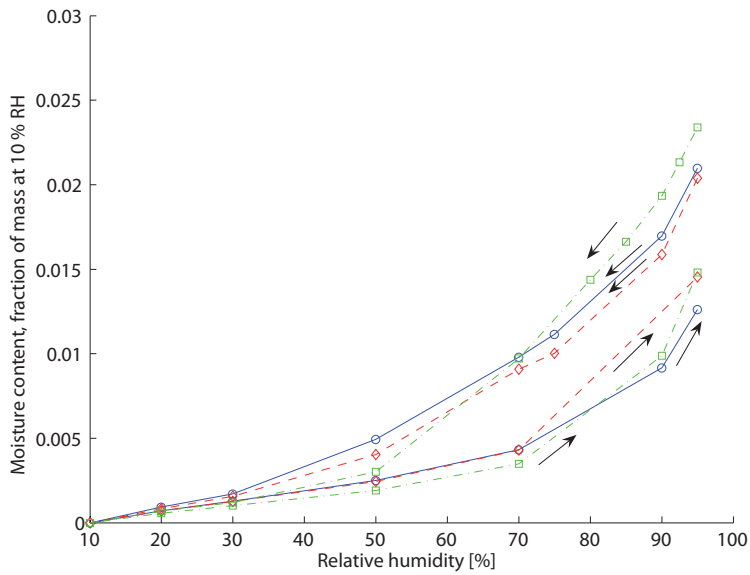

Figure 4.9: Sorption isotherms determined for three samples of material SFC, Floor 4310 Fibre Flow.

4.3 Scanning curves

In each of the first test series, two scanning curves were obtained by two sections of linearly increasing/decreasing RH, ramp, one starting from the desorption isotherm and the other from the absorption isotherm. This method was previously used for determining scanning curves for self-levelling flooring compounds [43]. The RH level was kept constant for a certain time before and after the scanning determination sequence, in order to achieve sample mass equilibrium.

However, as equilibrium, in a strict sense, was not obtained no matter how long RH was kept constant, the scanning ramp initially became disturbed by a mass loss/gain, see Figure 4.10. In Figure 4.10 the x-axis represents time in

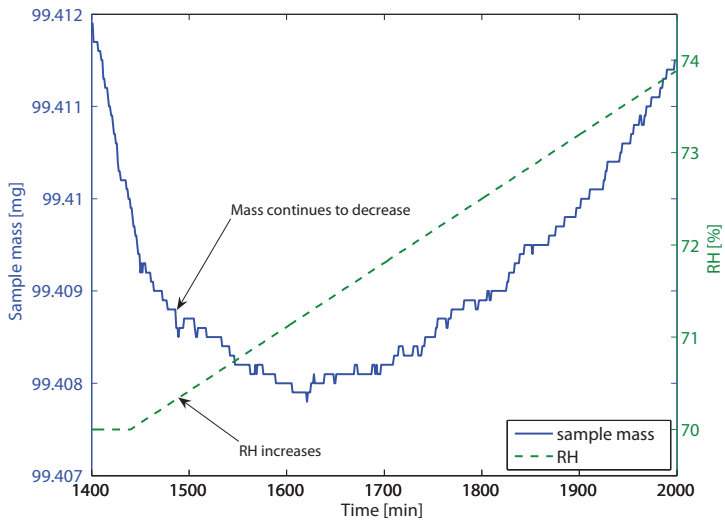

Figure 4.10: Equilibrium is not obtained before the RH ramp starts at 1440 min and 70 % RH.

minutes, the left hand y-axis represents sample mass in mg and the right hand y-axis represents RH in % RH. As can be seen in Figure 4.10 the sample mass, solid line, still decreases beyond 1440 minutes, even though the generated RH increases, dashed line. Therefore a time lag effect was obtained. In addition, the error increased even more as the curve fitted asymptotic mass was used.

This effect was compensated for by linearly superimposing the difference between the recorded and asymptotic mass, thereby reducing the error. Unfortunately, it was not feasible to apply curve fitting according to Eq. (4.1) on

scanning sections determined from a linearly increasing/decreasing RH. Instead a calculation was performed to compensate for the time lag effect obtained, by linearly superimposing the difference between recorded and asymptotic mass. The curve fitting method, time lag compensation, and the sorption isotherms obtained are presented in detail in Paper III.

The test sequence for scanning curve determination was modified by inserting a step wise RH change before the gradual RH change see Figure 4.11. In this way it was possible to compare a scanning curve evaluated by using Eq. (4.1) with a scanning curve obtained by using the time lag compensation evaluation. The results from this investigation clearly show that the scanning curve slope in-

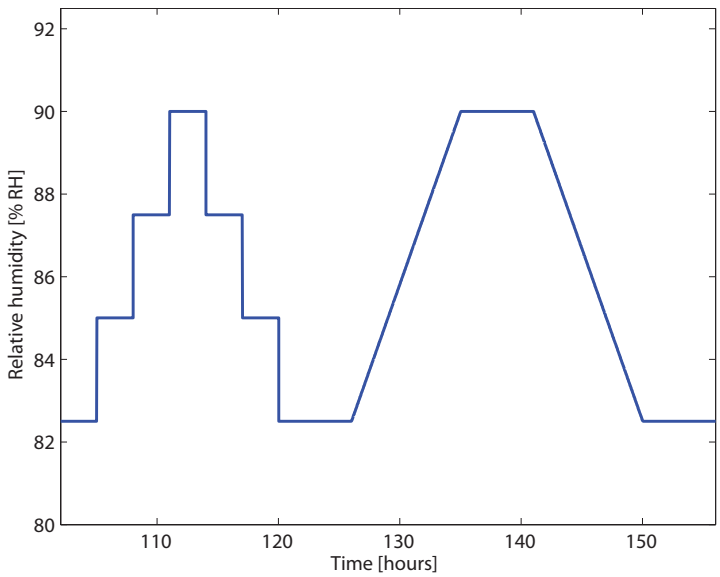

Figure 4.11: Detail of test sequence for comparing one scanning curve obtained by stepwise RH-changes with a scanning curve obtained by gradual RH-changes.

creases faster by using the stepwise RH changing method, see Figure 4.12. The scanning curve obtained by using the recorded sample mass, dashed line, contain less moisture compared with the scanning curve obtained by using the time lag compensation, solid line. In turn, the scanning curve obtained from stepwise changes to the ramp, dash dotted line, contains more moisture compared with the time compensated scanning curve obtained from the ramp.

In order to decrease possible remaining time lag effects, the previous method was further developed in the later test series. By replacing the RH ramps in

the test sequence with a sequence of small discrete RH steps, potential time lag effects were minimized. Thus the attained scanning curves were less affected by the non-existing equilibrium caused by earlier RH steps.

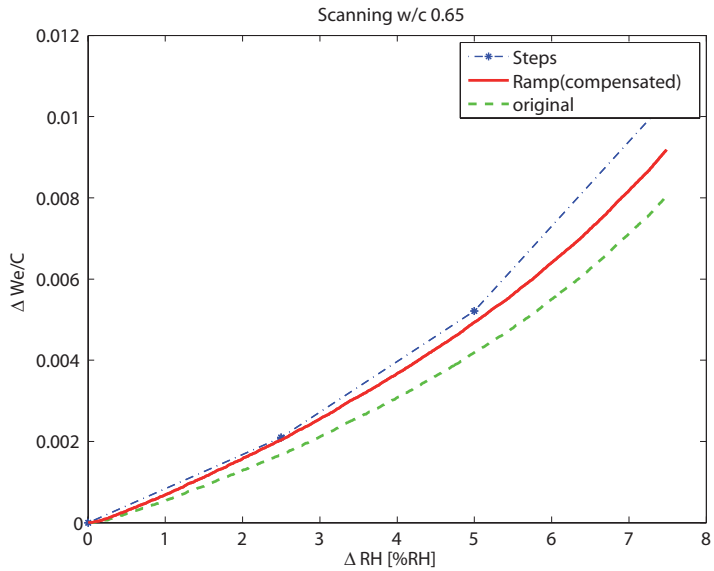

Figure 4.12: A comparison of the absorption scanning curves determined by using untreated data, a gradual RH change (time lag compensated), and a stepwise RH change, dashed, solid, and dash dotted line respectively. The point of origin represents the starting points at the desorption isotherm where scanning starts.

These new sets of scanning curves all started only from the desorption isotherm. In addition, the scanning absorption curves were directly followed by a desorption scanning curve, thus forming a small loop inside the main boundary loop. This approach was chosen, as such a sequence of moisture changes may occur at the top surface of a concrete slab when a screed is applied.

Figure 4.13 gives an example that illustrates where the different scanning curves are located with reference to the sorption isotherm.

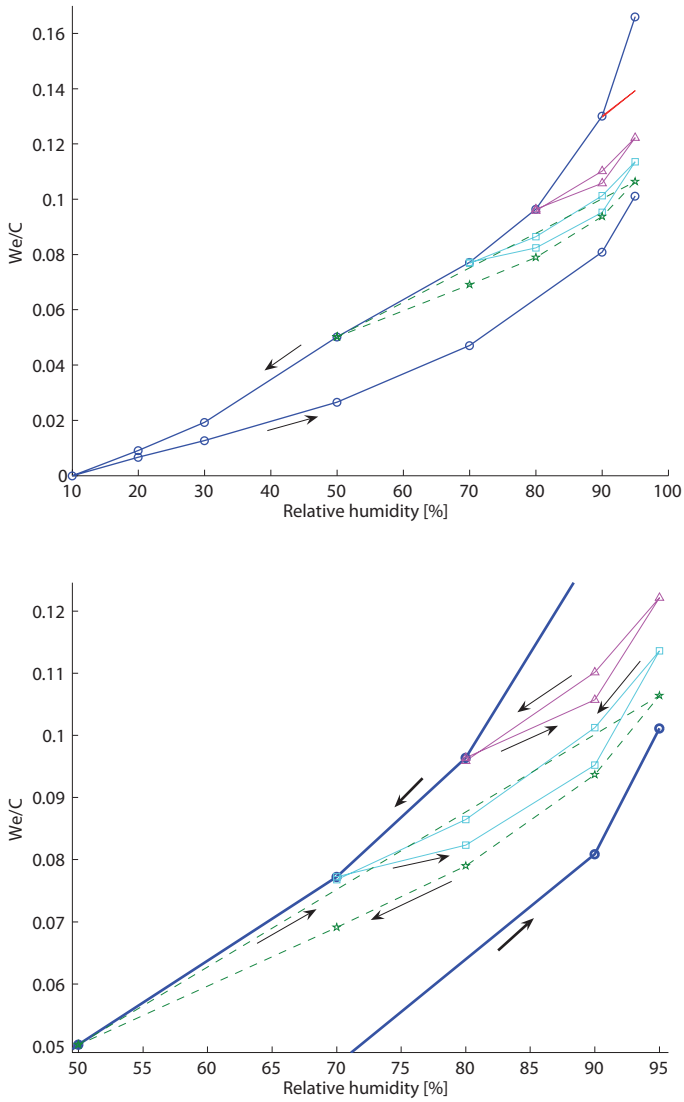

Figure 4.13: The top diagram shows the absorption and desorption isotherm of a w/c 0.65 concrete including a number of sequential scanning curves starting at different RH, 90, 80, 70 and 50 % RH. This sample is taken 20 mm from the slab base. The bottom diagram shows a detail of the achieved scanning curves where arrows indicate whether absorption or desorption scanning are determined.

Absorption scanning curves

To be able to show the scanning curves in detail, curves for different starting points on the desorption isotherm have been combined into one diagram from the starting point at the desorption isotherm.

Figures 4.14 - 4.17, display absorption scanning curves starting from RH_0 on the desorption isotherm for each separate material. Curves marked RH_0=82.5 are not "pure" absorption scanning curves. Originally they started scanning at 80 % RH, but experienced a number of inner absorption/desorption scanning cycles before starting at 82.5 % RH, inner scanning.

The x-axis in Figures 4.14 - 4.17, represents the change in RH. The y-axis in Figures 4.14 - 4.16, represents the change in We/C. In Figure 4.17, the y-axis represents the change in moisture content. The starting point of each scanning curve is indicated as RH_0 at the end of each displayed absorption scanning curve. Line markers indicate the determined We/C with reference to the starting point. The dashed line in Figure 4.14 suggests an estimated absorption scanning curve beginning from 50 % RH, since the moisture content was not determined at intermediate RH steps.

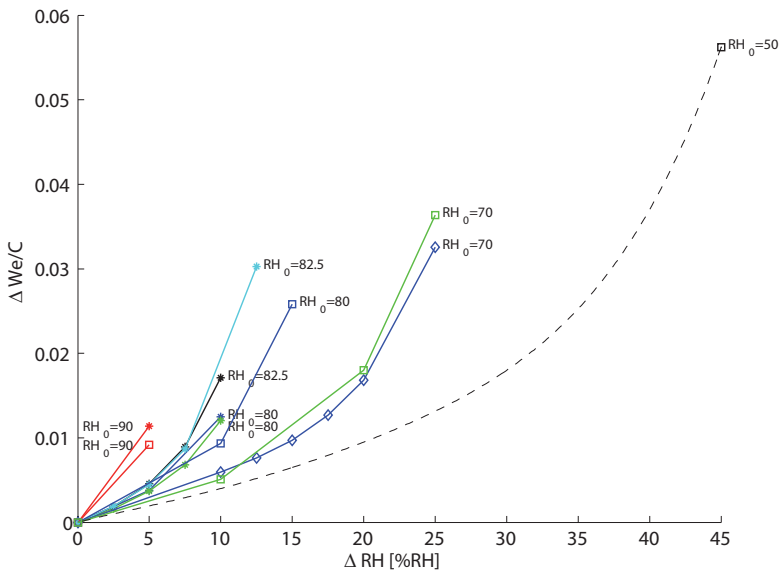

Figure 4.14: Absorption scanning curves for three samples of w/c 0.65 concrete, material C, expressed as changes in We/C and RH from the starting point RH_0 of the desorption isotherm. The three line markers stars, squares, and diamonds represent three separate samples.

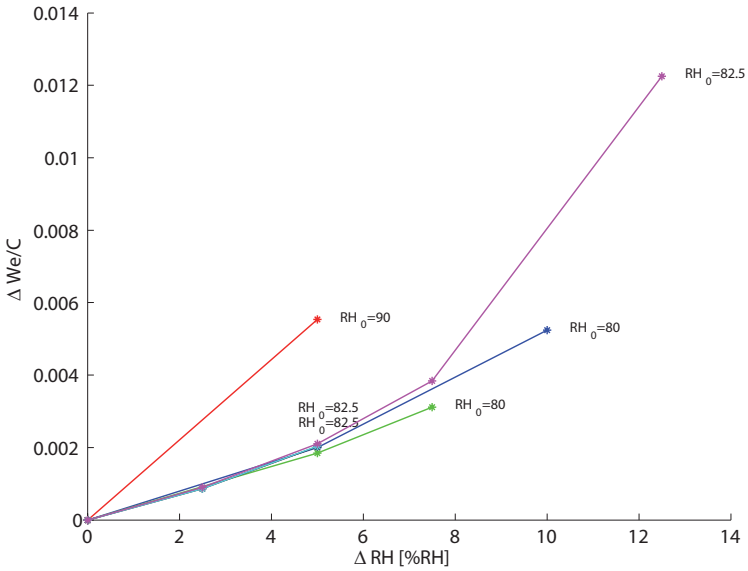

Figure 4.15: Absorption scanning curves determined for one sample of w/c 0.40 concrete, material C_{HCS}.

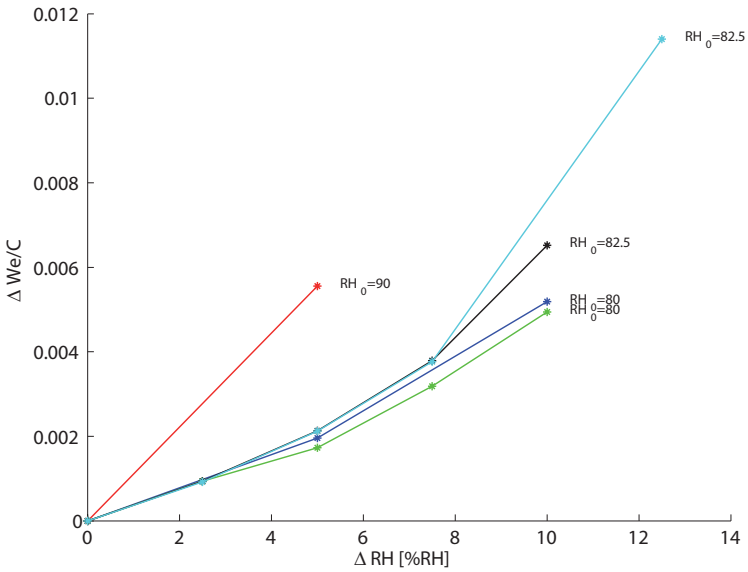

Figure 4.16: Absorption scanning curves determined for one sample of w/c 0.55 cement mortar, material M.

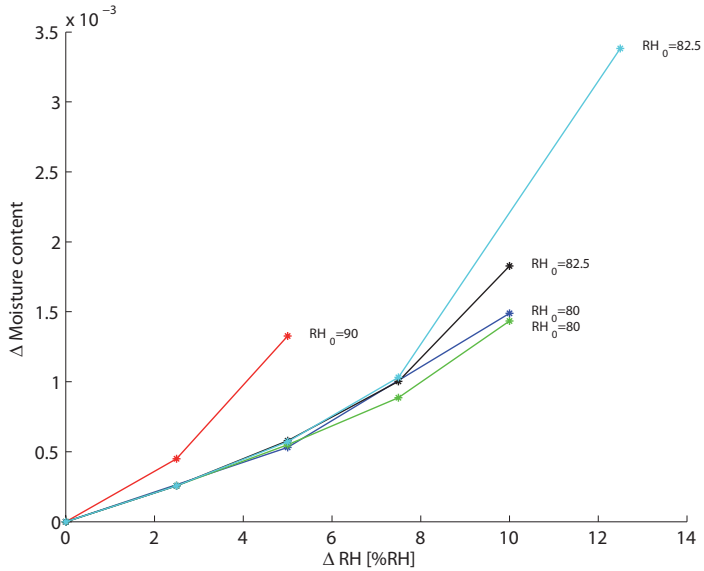

Figure 4.17: Absorption scanning curves determined for one sample of Floor 4310 Fibre Flow, material SFC.

There is a clear relationship between the absorption scanning curves obtained and the starting point on the desorption isotherm. The slope of an absorption scanning curve starting at a lower RH is shallower than a slope starting from a higher RH level. In addition the scatter of the absorption scanning curves is low.

The absorption scanning curves obtained at a starting point of 90 % RH appear to be linear, in Figures 4.14 - 4.16. Such results were obtained since the moisture content was not determined for intermediate RH levels.

Desorption scanning curves

Desorption scanning curves are shown in a similar manner as the absorption isotherm, with the starting point of the absorption scanning curve as a common reference.

Figures 4.18 - 4.21, display desorption scanning curves starting from the end point of a prior absorption scanning curve. The x-axis in Figures 4.18 - 4.21, represents the change in RH from that starting point. The y-axis in Figures 4.18 - 4.20, represents the change in We/C. In Figure 4.21, the y-axis represents the change in moisture content. RH_0 defines the starting point on the preceding absorption scanning curve, line markers indicate the We/C obtained.

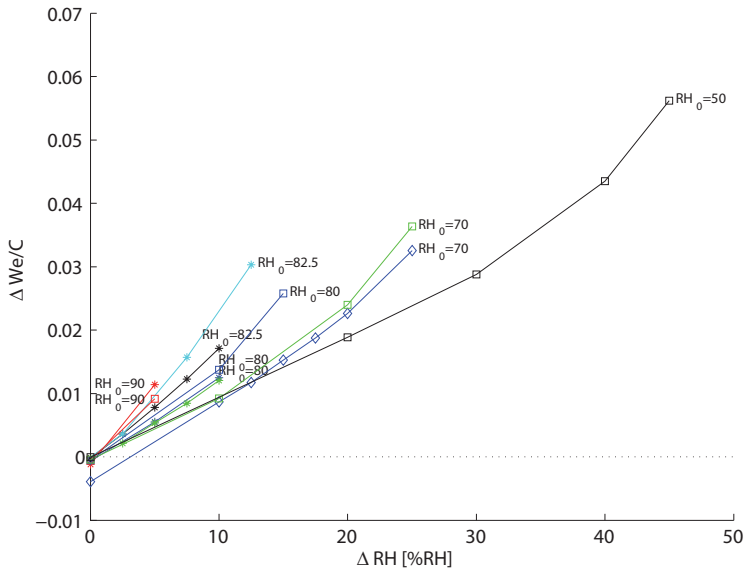

Figure 4.18: Desorption scanning curves starting from the absorption scanning curve for w/c 0.65 concrete, material C, expressed as changes in We/C and RH from the starting point RH_0 of the absorption scanning curve.

The determined desorption scanning curves clearly show that they are dependent on the starting point RH, RH_0. In addition most of the desorption scanning curves approximately end on the starting point. This suggests that an absorption scanning curve taking off from the desorption isotherm at a particular moisture content returns to the starting point, thus closing the loop. The path back is dependent on where the absorption ends and desorption starts. The above may imply that if a complete saturation occurred when absorbing moisture, then the desorption scanning curve would follow the desorption isotherm

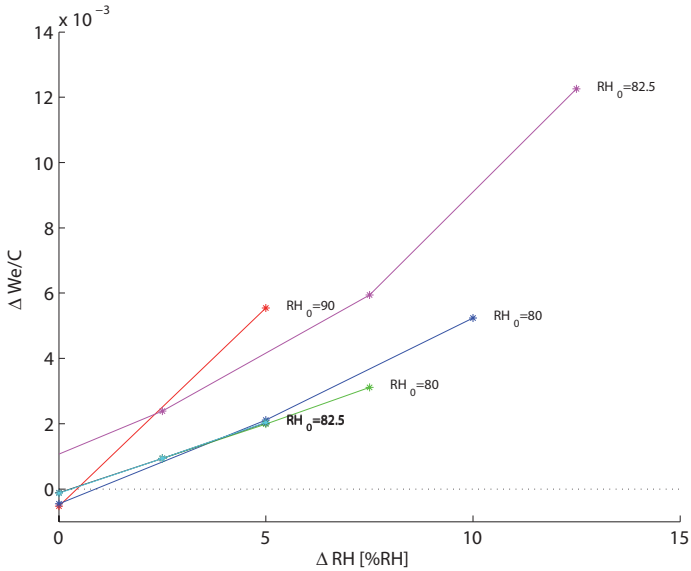

Figure 4.19: Desorption scanning curves starting from the absorption scanning curve for w/c 0.40 concrete, material C_{HCS}.

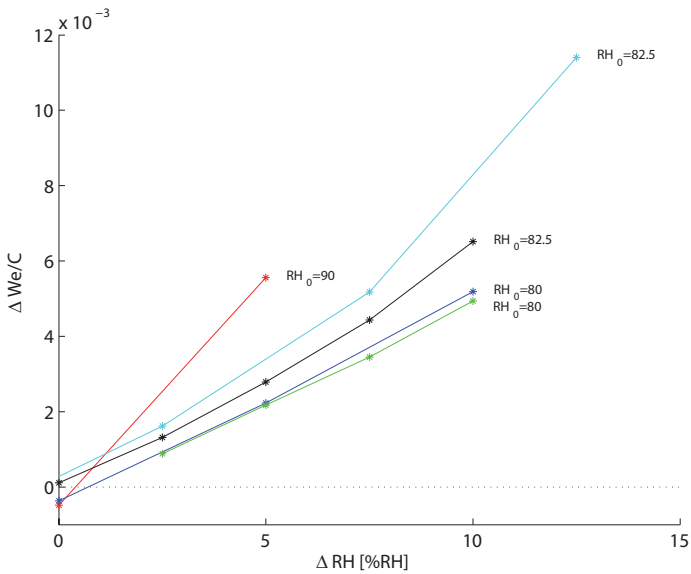

Figure 4.20: Desorption scanning curve starting from the absorption scanning curve for w/c 0.55 cement mortar, material M.

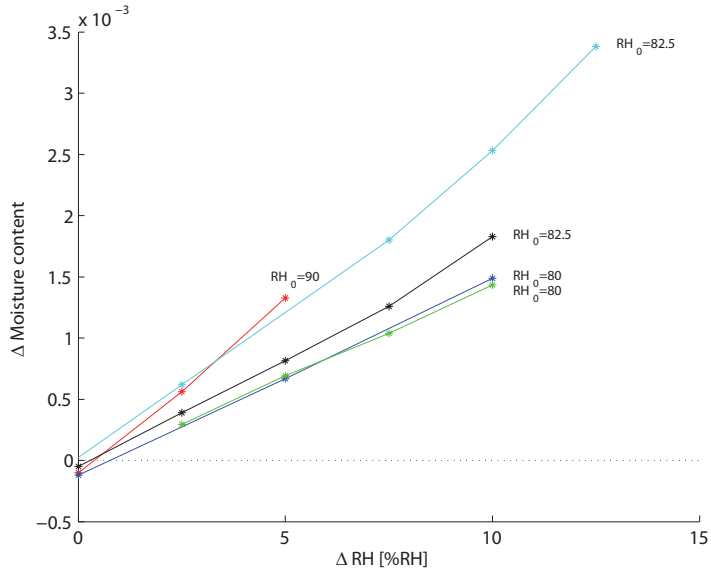

Figure 4.21: Desorption scanning curve starting from the absorption scanning curve for Floor 4310 Fibre Flow, material SFC.

when returning to the starting point provided there was no change in material characteristics, i.e., hydration would occur throughout the saturation procedure. This may not be true for the 1^{st} desorption isotherm, however.

4.4 Moisture transport properties

Moisture redistribution through a screeded concrete slab is slow. Therefore it may take a long time to reach a complete redistribution. When flooring is applied early on a moist screed, thus achieving an uneven moisture distribution, the model may underestimate the actual humidity obtained beneath the flooring, because the ”local” redistribution in the screed is much faster than the overall redistribution in the whole slab. To be able to quantify these effects, moisture transport properties must be known. However, moisture transport properties were not included in the quantitative model described in section 3.3. Moisture transport coefficients were determined in order to illustrate possible differences in the materials used, to be used if such considerations were to be included in future model development.

Moisture transport coefficients were determined for C, M, SFC, and coated plywood by using the cup method. This method is based on moisture loss determinations performed on closed impermeable vessels, where the top is ”sealed” with the investigated semi-permeable material. The cup is stored in a climate room where the surrounding climate is kept constant at 55 % RH and 20 °C.

A small container of saturated salt solution is put inside the vessel, see Figure 4.22. The mass of each vessel is determined on a calibrated balance, hence monitoring the expected mass loss. Several humidity levels may be achieved inside the vessel by using a number of different salt solutions.

In this study five different salt solutions were used to generate a specific RH at 20 °C [44], see Table 4.3.

Table 4.3: Salt solutions with deionized water and the generated RH.

Salt solution	NaBr	NaCl	KCl	KNO_3	K_2SO_4	H_2O
RH [% RH at 20 °C]	59.1	75.1	85.1	94.6	97.6	100

Cylindrical samples of w/c 0.65 concrete, w/c 0.55 cement mortar, and Floor 4310 Fibre Flow, were extracted from Batch 1 by using a water lubricated core drill. These cores were subdivided into 13 - 20 mm thick discs by using a wet saw, in order to separate screed from concrete material and to obtain smooth specimen surfaces. The mean diffusion coefficients for w/c 0.65 concrete were determined by using four to nine discs per each salt solution. Furthermore, the mean diffusion coefficients for the two screeds were determined by using one to two discs per each salt solution.

The mean diffusion coefficients for plywood were determined on three discs per each salt solution. The mean flows were calculated and used to calculate

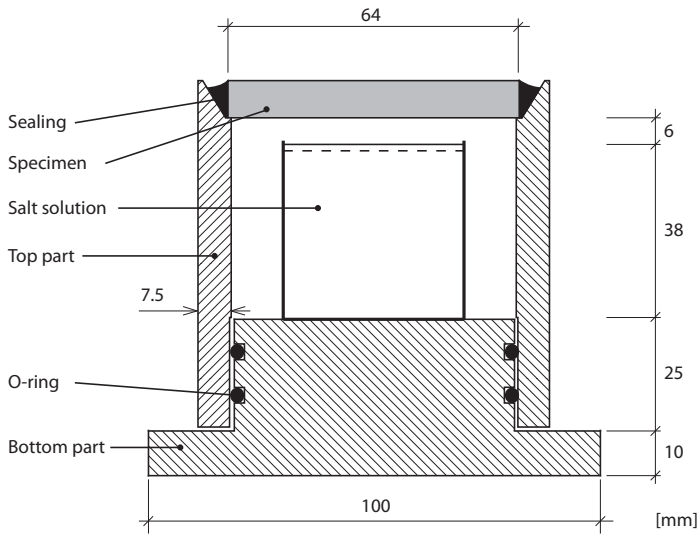

Figure 4.22: Illustration showing the cup used to determine diffusion coefficients of materials C, M, SFC and coated plywood.

the resistance of the air layer between the salt solution surface and the base of the specimen, thus obtaining the actual boundary RH. The final evaluation of average diffusion coefficients was performed by using a method described in [45].

Diffusion coefficients for the flooring material, Tarkett Eminent, were determined on one sample per each RH level, by using glass cups with a larger diameter, 183 mm, to reduce possible edge effects and increase the resolution.

The results of the evaluated mean diffusion coefficient for the w/c 0.65 concrete, the w/c 0.55 cement mortar and Floor 4310 Fibre Flow are shown in Figure 4.23. The mean diffusion coefficient between 55 % RH and 60 % RH seems too low in comparison with the higher levels. This is possibly either a consequence of the low difference between the outside and the inside climate or an error in the generated 55 % RH climate.

The mean diffusion coefficient of the PVC flooring material shown in Figure 4.24 is two orders of magnitude lower than that for the cement based materials, thus it is much less permeable than those materials. The mean diffusion coefficient at 55 to 75 % RH also seems too low compared with the coefficients obtained at a higher humidity. The flooring cups were stored in the same room as the concrete sample cups, it is therefore possible that the relative humidity was other than 55 % RH.

The mean diffusion coefficients for coated 13 mm plywood, determined on

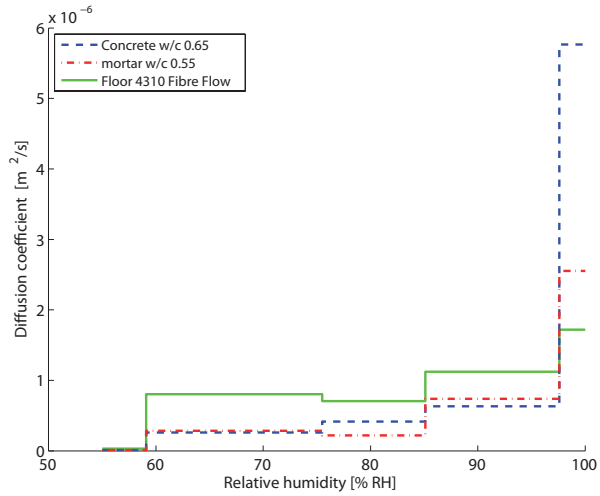

Figure 4.23: Mean diffusion coefficient of material, C, w/c 0.65 concrete, M, w/c 0.55 cement mortar, and SFC, Floor 4310 Fibre Flow. The diffusion coefficient was determined in the interval 55 - 100 % RH.

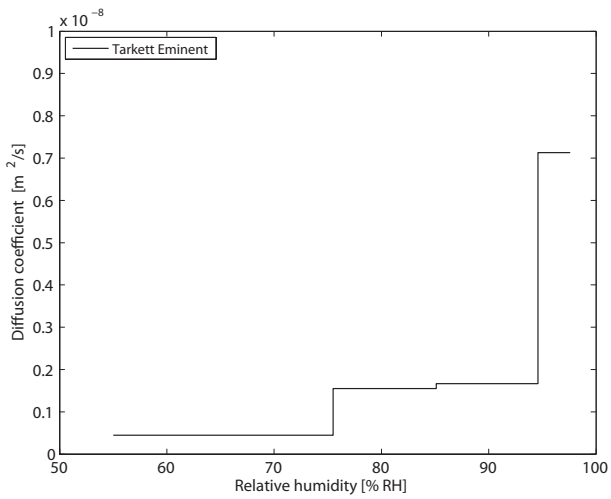

Figure 4.24: Mean diffusion coefficient of a Tarkett Eminent, 2 mm, homogeneous PVC flooring. The diffusion coefficient was determined in the interval 55 - 97.6 % RH.

three discs per salt solution shown in Figure 4.25, are of the same magnitude as for the cement based materials. The mean diffusion coefficient in the 55 - 60 % RH range, in this case also, is unexpectedly low. The plywood sample cups

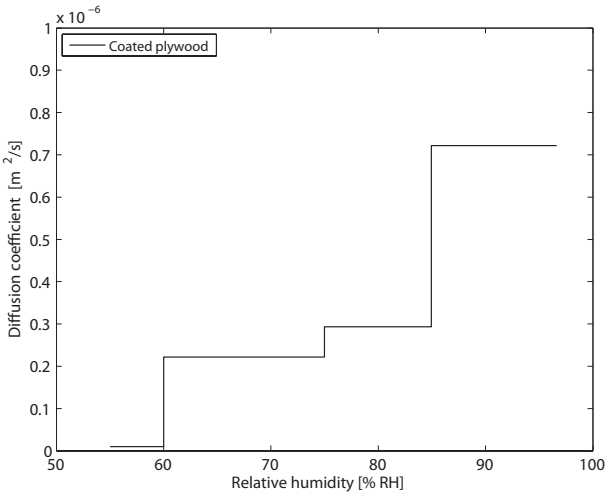

Figure 4.25: Mean diffusion coefficient for coated plywood 13 mm, used as formwork. The diffusion coefficient was determined in the interval 55 - 97.6 % RH.

were stored in the same climate room as the concrete sample cups, thus the low mean diffusion coefficients may be explained correspondingly.

4.5 Redistribution of moisture after early drying

Redistribution of moisture in a newly cast and somewhat dried concrete floor structure causes an increase in humidity at the concrete - adhesive interface. This humidity increase may adversely affect materials in contact with the concrete floor and contribute to deterioration, e.g. adhesive degradation [46, 47]. It is therefore important to limit the moisture content of the concrete by drying, or limit its exposure to external moisture sources. If it is not properly dried there is a risk of material deterioration. All measures that may prevent such an increase are therefore of interest.

Results from two independent studies showed unexpectedly low humidities below the sealed surface after redistribution [48, 49]. Additional, long-term self desiccation was one mechanism that was suggested to explain the large decrease in humidity below the flooring. If drying starts immediately after casting, the humidity in the concrete surface region decreases. This will limit the time for hydration under optimum humidity conditions, i.e. when enough moisture is present. The less hydrated cement in the surface region may react further with the later redistributed moisture from the slab base and increase its degree of hydration, thereby decreasing the humidity. However, the authors were not able to validate the suggested explanation for these interesting findings with available data.

An experiment was designed to repeat the findings shown in the two previous studies and test the model in section 3.4. Special attention was given to match the moisture distribution before the surface was sealed, to attain sufficient accuracy in RH measurements, and to monitor possible leakage. In addition it was important to rapidly reduce the humidity to less than 80 % RH in the upper part of the concrete, in order to hinder further hydration. This was accomplished by using a concrete with a w/c ratio of 0.65. The mix specification is shown in Table 4.4.

Table 4.4: Mix specification for the concrete used in the study of effects of early drying of humidity. Quantities are presented in kg/m^3.

Material	C
SH cement, CEM I 52.5 R	250
Water	162.5
Dry sand 0-8 mm	976.4
Dry gravel 8-12 mm	976.4

The theory of the impact of early drying was tested by comparing two drying treatments applied to w/c 0.65 concrete prior to sealing the surface, i.e. flooring. One population was dried directly, one day after curing, and the other was sealed 30 days before drying at 55 % RH and 20 °C. Each sample consisted of a 100 mm thick and 310 mm wide concrete cylinder, which was poured in a 20 mm thick polypropylene form. The moisture distribution was determined on all specimens by using calibrated Vaisala RH sensors. These were installed through drilled holes equipped with inserted 80 mm long plastic tubes. The centre of the sensor was located at a distance of 20-55 mm from the drying surface, with a distance of 5 mm between each sensor, see Fig 4.26.

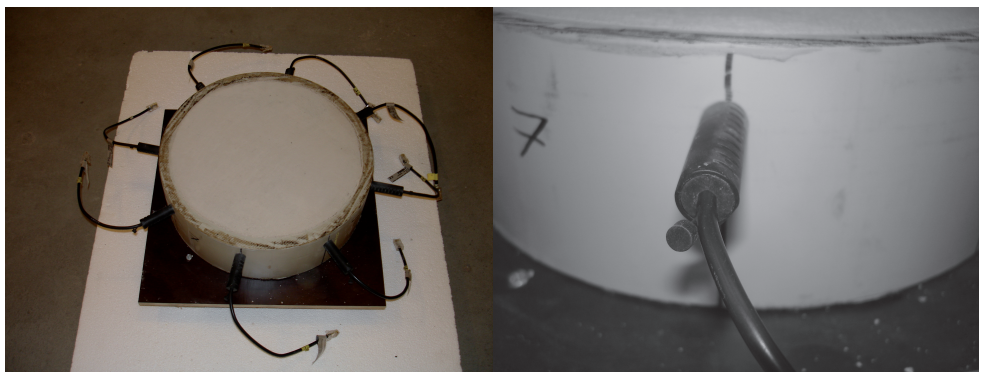

Figure 4.26: A concrete specimen with attached moisture sensors is shown to the left. A close-up of the rubber plug seal at the sensor cable is shown to the right.

Batch 1 was allowed to dry for 59 days prior to sealing. At this time the sensor with the centre 20 mm from the surface showed a reading of 80 % RH or less. This reading demonstrated that the upper 20 % of the concrete cylinder, at least once during drying, was exposed to a humidity that limits hydration. Batch 2 was sealed once the mean moisture distribution (at all depths) was found to match the mean moisture distribution determined just before sealing Batch 1, within an accuracy of $\pm$ 1 % RH.

After drying, the moisture in the specimens was allowed to redistribute for nearly 3 months. Subsequently the internal moisture distribution was determined including the humidity directly under the seal. This was done to establish that redistribution was completed, indicated by a uniform RH distribution through the specimen, see Figure 4.27. The humidity under the seal in Batch 1 was compared with the humidity in Batch 2 using a two sample student t-test.

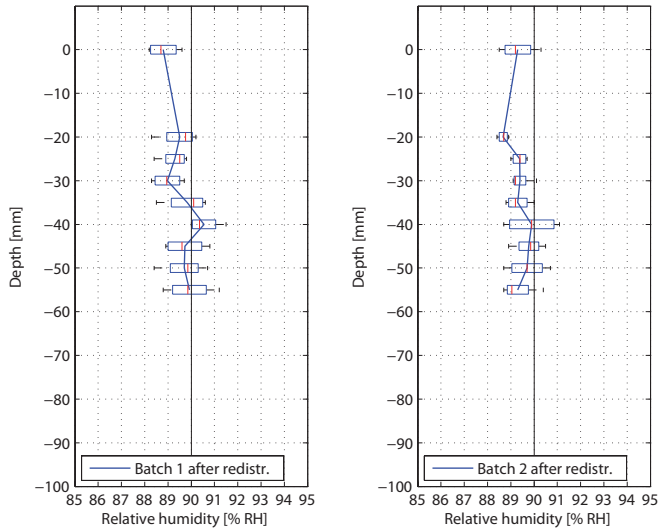

Figure 4.27: The moisture distribution after redistribution in Batch 1 is shown to the left and that in Batch 2 is shown to the right. On each box, the central mark is the median and the edges of the box are the 25^{th} and 75^{th} percentiles. The lines from the ends of the box (whiskers) extend to the most extreme data points considered not to be outliers.

The test showed that there was no significant difference in mean humidity between the two batches tested on a significance level of 5 %. A more detailed description of the method and results is found in Paper VI.

4.6 Critical limit for ion transport

Ion transport is an important factor for the durability in several applications. Here, alkaline deterioration of adhesives under a PVC flooring is in focus. Therefore, alkali is used when studying ion transport. Redistribution of potassium was determined on mortar specimens exposed to a certain drying treatment. The mix specification for the two mortars is described in Table 4.5.

Several sets of five specimens were first dried at 55 % RH and 20 °C for various periods, see Figures 4.28A and 4.29A. This 1^{st} drying lowered the average moisture state to a variable degree, represented by the solid curved line, see Figures 4.28A and 4.29A. A longer drying period obviously generated a lower average humidity. Then the specimens were sealed to allow redistribution to occur, until a uniform moisture distribution in terms of RH was reached, represented

Table 4.5: Mix specification for the materials used in the ion transport investigation. Quantities are presented in kg/m^3.

Material (w/c)	L (0.4)	H (0.65)
CEM I 52.5 R	702	333
Water	281	217
CEN-Standard sand EN 196-1 0-2 mm	1199	1602

by the dashed line, see Figures 4.28B and 4.29B. Redistribution was judged to be finalized when the RH (RH_{0-1} and RH_{0-2}) at both sides were equal, within an accuracy of $\pm$ 0.5 % RH.

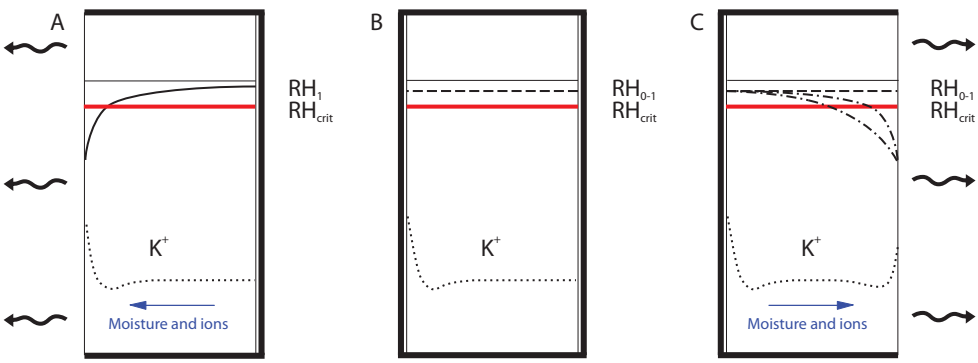

Figure 4.28: Illustration of the humidity and alkali distribution in a concrete specimen subjected to 1st (left) and 2nd (right) drying. The humidity level after redistribution, RH_{0-1}, is above the critical limit for ion transport.

The drying treatment does not generate a uniform distribution in terms of moisture content, see Figure 4.30B. In the left half of the specimen facing the earlier open side, the moisture content is on average less than the moisture content in the second half. The moisture content reaches its lowest level at the surface and increases with depth until reaching a maximum. This appearance is explained by the hysteresis and the scanning curves that govern the gain in moisture content when moisture is redistributed and reaches the earlier dry half.

On the contrary, the other half of the specimen has experienced only drying, see Figure 4.30B. This means that all parts in this half have reached their moisture state by tracking a pure desorption isotherm. Therefore both moisture content and RH distribution are uniform on this side. The point at which the material

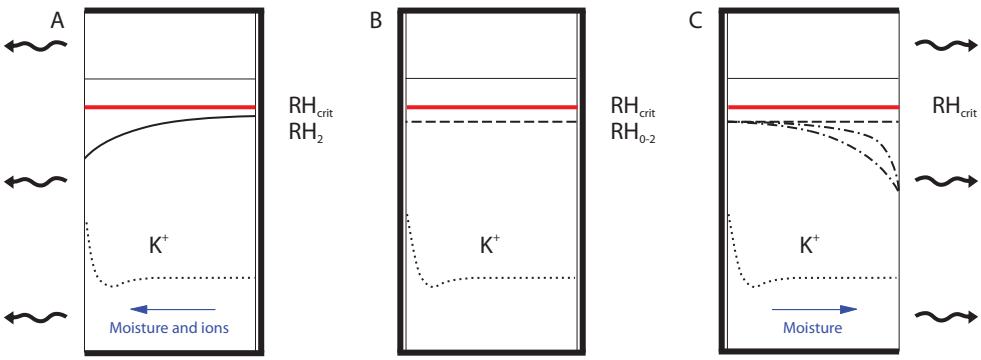

Figure 4.29: Illustration of the humidity and alkali distribution in a concrete specimen subjected to 1^{st} (left) and 2^{nd} (right) drying. The humidity level after redistribution, RH_{0-2}, is below the critical limit for ion transport.

has experienced both drying and wetting is about half of the specimens thickness. This fact is clearly demonstrated in Paper VI.

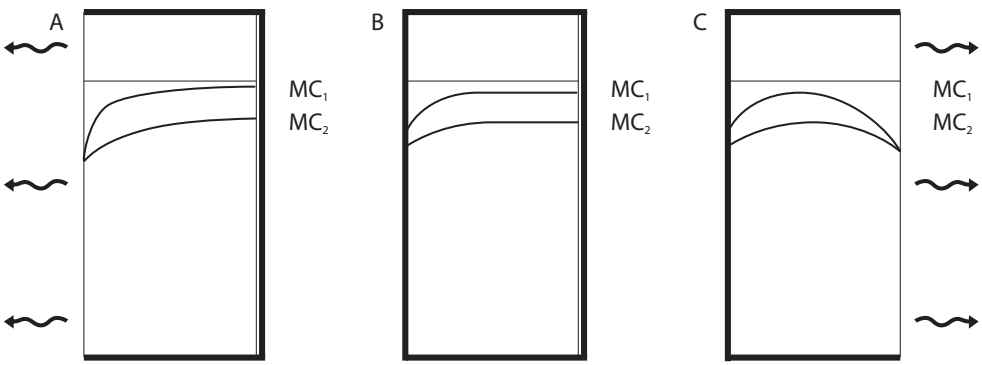

Figure 4.30: Illustration of the moisture content distribution, MC_1 and MC_2, in a concrete specimen subjected to 1^{st} (left) and 2^{nd} (right) drying at two humidity levels, RH_{0-1} and RH_{0-2}, shown in Figure 4.28 and Figure 4.29.

The drying treatment continues, on three of the five specimens, with a 2^{nd} drying at 55 % RH and 20 °C. The 2^{nd} drying is applied after establishing the end of moisture redistribution, but this time by opening the other side, see Figures 4.28C and 4.29C. At this point the flow of moisture is reversed. Drying

now occurs, to the right, from a lower moisture level. It is possible to obtain any humidity level lower than the humidity achieved by self-desiccation, by initial drying at various durations and climates.

The method used to redistribute moisture is designed to initiate alkali redistribution by convective moisture flow in two steps, the 2^{nd} being the most important. The 1^{st} applied drying causes an increase in alkali concentration at the drying surface, see dotted curve in Figures 4.28A and 4.29A. This increase is mainly the result of a moisture flow, since there is no driving potential for alkali diffusion at the start. As soon as the alkalis accumulate at the surface there will be a driving potential in the direction opposite to the moisture flow governed by RH differences. However, the moisture content is significantly reduced at this position and thereby limits the possibility of moving alkalis in the opposite direction by diffusion, see Figure 4.30A. The moisture content is still less than in the specimen half facing the sealed side, even after a complete redistribution of moisture, see Figure 4.30B. Therefore this limiting mechanism is still present after moisture redistribution, however to a slightly reduced extent.

The 2^{nd} drying step is applied to initiate alkali redistribution in the right half of the specimen via the moisture flow from a certain moisture state, see Figures 4.28C, 4.29C and 4.30C. As stated earlier, both moisture content and RH distribution are at first uniform in this part, see Figures 4.28B, 4.29B and 4.30B. In addition the alkali distribution is at first likely to be uniform, see dotted curve in Figures 4.28B and 4.29B. This assumption rests on the fact that moisture flow, up to this point, has only occurred at a low magnitude in this part of the specimen. Furthermore, there is no apparent cause of achieving diffusion of alkali ions because differences in alkali content in this half of the specimen are insignificant.

Alkali distribution was established by running four specimens for each mortar and RH level in an SEM-EDS instrument. One specimen was dried at one side only and this served as a reference. The data obtained from the SEM-EDS measurement was treated by using Matlab. This method is described in detail in Paper VII. One typical result after application of the data treatment is shown in Figure 4.31.

Figure 4.31 shows the alkali distribution in four different samples of w/c 0.65 mortar, one subjected to the 1^{st} drying only (upper left) and three specimens subjected to the whole drying treatment. The potassium content is shown on the y-axis and the x-axis represents the average position of the SEM-EDS analysis image, in mm, with reference to the surface subjected to the 2^{nd} drying (the right hand side in each diagram). The average potassium content in each image is represented by the thin solid curve and is quantified as the wt.-%. The average

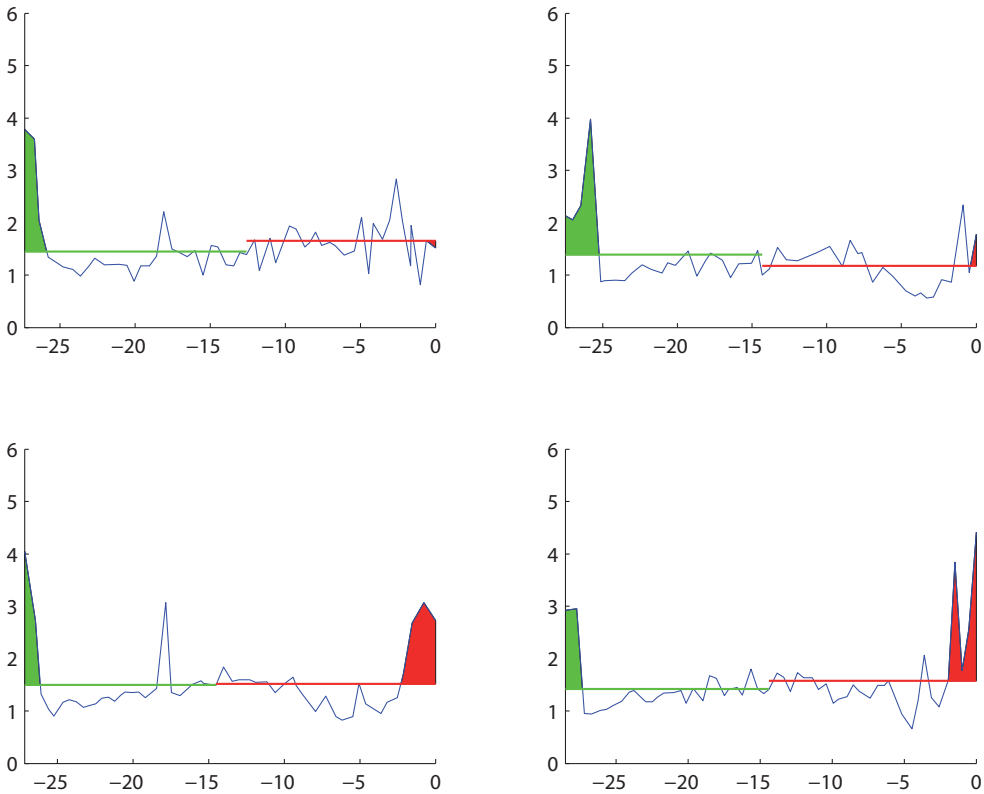

Figure 4.31: Alkali redistribution at 85 % RH, reference in upper left corner.

content through half of the specimen, right and left, is shown as a solid horizontal line. The green area to the left shows the accumulation of alkali achieved after applying the 1^{st} drying and the red area to the right the accumulation achieved after applying the 2^{nd} drying.

The study clearly shows that ions accumulated during the 2^{nd} drying at a humidity level of 78 % RH obtained by drying in w/c 0.65 mortar. This is strong evidence that the critical humidity level for convective ion transport is less than 78 % RH in w/c 0.65 mortar. Ion accumulation was also shown to occur in w/c 0.4 mortar at the 2^{nd} drying at a humidity level of 91 % RH obtained by drying. This implies that convective ion transport occurs at a level of 91 % RH in w/c 0.4 mortar.

For additional results of the ion content distribution after the 2^{nd} drying including the standard deviation see appendix.

Chapter 5

Model validation

Moisture distributions were determined for nine screeded slabs on several occasions before and after flooring, see Paper IV. The future moisture profiles were evaluated by using the proposed method in chapter 3. Each diagram in Figures 5.1 - 5.5 shows the screeded slab's moisture distribution before flooring, dashed lines, and after a certain time of redistribution, thick solid lines. In addition, the evaluated uniform RH level is shown as a thick dashed line in each diagram. In slabs 5-8 one additional moisture profile per each screeded slab was determined after the publication of Paper IV, therefore these do not appear in Paper IV. It was not possible to perform this analysis on the homogeneous slabs investigated in Paper VI, because of incomplete data.

The iteration procedure is shown in Table 5.1, where slab 4 serves as an example.

The moisture distribution in slab 4 determined before flooring application shows that the humidity varies between 75.5 % RH at section 0.00-0.02 m, and 86.5 % RH at section 0.06-0.08 m, see Table 5.1. The initial guess of the uniform moisture distribution according to the quantitative model is 83.75 % RH, see Table 5.1.

The determination of the moisture capacity in each section is dependent on both the moisture history and its level with reference to the initial guess. The moisture capacity in each section of material C is determined by using the desorption isotherm for sections where the determined RH is above the initial guess, see section 4.2 Figure 4.6, apart from section 0.04 - 0.06 m. Section 0.04 - 0.06 m has to be carefully investigated since it is close to the screed. This section is likely affected by application of the wet screed before reaching the obtained humidity.

Table 5.1: The calculation of the future uniform moisture distribution inside a screeded concrete slab is performed according to the quantitative model presented in section 3.3.

			1^{st} iteration		
Depth	d_i	$\overline{\varphi_i}$	$\left(\overline{\frac{dW_e}{d\varphi}}\right)_i$	$d_i \cdot \left(\overline{\frac{dW_e}{d\varphi}}\right)_i$	$d_i \cdot \left(\overline{\frac{dW_e}{d\varphi}}\right)_i \cdot \overline{\varphi_i}$
[m]	[m]	[% RH]	[kg/m^3]	[kg/m^2]	[kg/m^2]
0.00-0.02	0.02	75.5	0.06	0.0012	0.0906
0.02-0.04	0.02	82.5	0.02	0.0004	0.033
0.04-0.06	0.02	85	0.3	0.006	0.51
0.06-0.08	0.02	86.5	0.8	0.016	1.384
0.08-0.10	0.02	86.5	0.8	0.016	1.384
0.10-0.12	0.02	86.5	0.8	0.016	1.384
$\sum$=				0.0556	4.7856
φ_∞ =		83.75		$Eq.(3.6) \Rightarrow$	$\frac{4.7856}{0.0556} = 86.1$

Slab 4 was subjected to drying at 60 % RH for a duration of 110 days before application of the M material which dried 90 days prior to flooring, see section 4.1 Table 4.2. This most likely implies that the humidity in section 0.04 - 0.06 m has first decreased on drying and later increased as a result of the screed application, cf. qualitative model Figure 3.2 point b. As the moisture distribution was determined 90 days after this application it is likely that the moisture capacity for section 0.04 - 0.06 m should be determined from the desorption scanning curve of material C. Therefore, the moisture capacity for section 0.04 - 0.06 m is determined from the desorption scanning curves, see section 4.3 Figure 4.18.

Furthermore, the moisture capacity in each section of material M is evaluated by using the absorption scanning curves, see section 4.3 Figure 4.16, since both sections will gain moisture to reach the guessed humidity level.

Equation (3.6) in section 3.3, gives a uniform humidity distribution of 86.1 % RH which is significantly higher than the initial guess. This increase in uniform humidity means that section 0.04 - 0.06 m now becomes drier than the new uniform humidity distribution, hence a 2^{nd} iteration may be needed. However, the increase in uniform humidity distribution to 86.1 % RH leads to a change in evaluating the moisture capacity from a desorption to an absorption scanning curve in section 0.04 - 0.06 m. Such a change in scanning implies an insignificant change of moisture capacity. Therefore, in this case a 2^{nd} iteration is unnecessary and better precision is not obtainable.

The result of using the quantitative model in each slab is shown in Figures 5.1 -5.5. In each diagram RH is shown on the x-axis and the vertical distance in mm from the slab surface is shown on the y-axis, positive figures for an increasing depth. The line markers represent the RH level obtained in each section. Flooring installation is defined as day 0 (zero) and the legend indicates when the profile was obtained in relation to flooring.

The different materials used for each screeded slab are indicated in the diagrams, C representing w/c 0.65 concrete, C_{HCS} representing w/c 0.4 concrete, SFC representing Floor 4310 Fibre Flow, and M representing w/c 0.55 cement mortar.

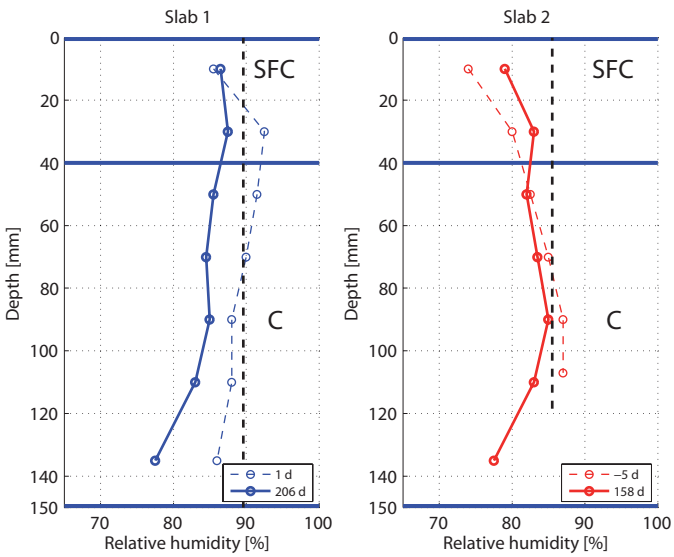

Figure 5.1: Moisture distribution determined for two SFC screeded concrete slabs on plywood at the time of flooring, thin dashed line, after complete redistribution predicted by the model, thick dashed line, and after x days of redistribution, thick solid line.

The humidity distribution determined 206 days after the flooring was laid in slab 1 indicates that the maximum RH is not yet reached, see Figure 5.1. The higher RH level obtained at the 30 mm level indicates that additional moisture will be transported upwards thus increasing the level by about 1 % RH. The results obtained from slabs 2 and 4, about 160 days after flooring, clearly demonstrate that moisture will be redistributed from the 30 mm level to the 10 mm level, see Figures 5.1 and 5.2. It is very likely that the future RH level be-

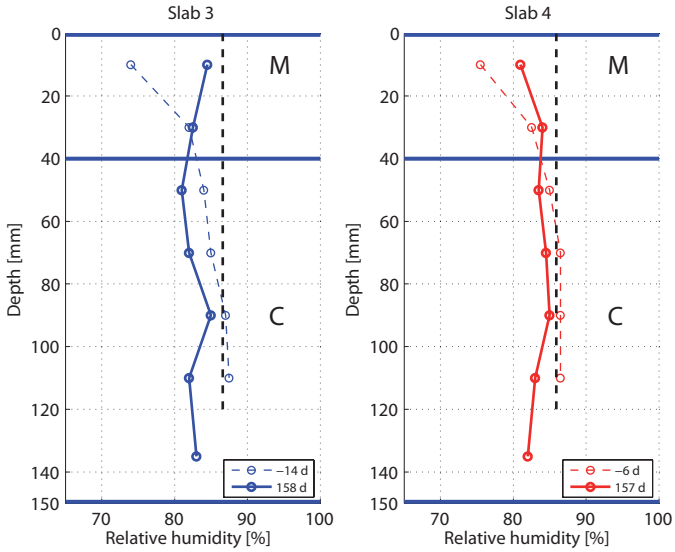

Figure 5.2: Moisture distribution determined for two M screeded concrete slabs on plywood.

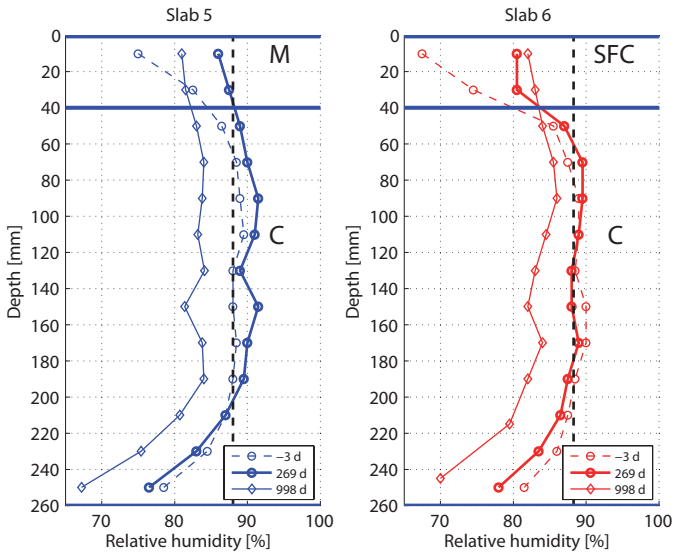

Figure 5.3: Moisture distribution determined for two of the M and SFC screeded concrete slabs.

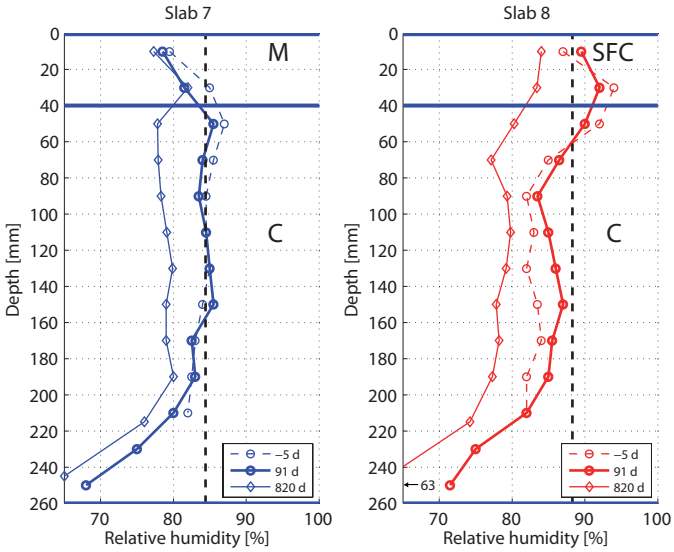

Figure 5.4: Moisture distribution determined for two of the M and SFC screeded concrete slabs.

neath the flooring will increase by about 3 - 5 % RH compared with the top RH levels obtained.

The determined RH distribution in slab 3 shows a higher RH level in the 0-20 mm section than in the 20-40 mm section, see Figure 5.2. This may be a consequence of measurement uncertainty as such an increase could not be explained by moisture redistributing from deeper sections.

Disregarding the expected future humidity increase, the proposed quantitative model gives results about 1 - 8 % RH on the safe side judging from slabs 1 - 4. However, including the expected future rise for slabs 1, 2 and 4 the overestimation drops to about 1 - 3 % RH.

Applying the quantitative estimation to slabs 5 and 6 results in a 2 - 7 % RH higher humidity at the 10 and 30 mm level determined 269 days after flooring, see Figure 5.3. However, on the basis of this moisture distribution a further increase in humidity is very likely to occur. Judging from the determined moisture distribution, the screed RH may increase by about 3 - 8 % RH. Including this future suggested increase the quantitative model underestimates the screed humidity by about 1 - 2 % RH.

When the quantitative model is applied to slabs 7 and 8, the screed humidity estimation is higher than that obtained for slab 7 and slightly lower for slab 8,

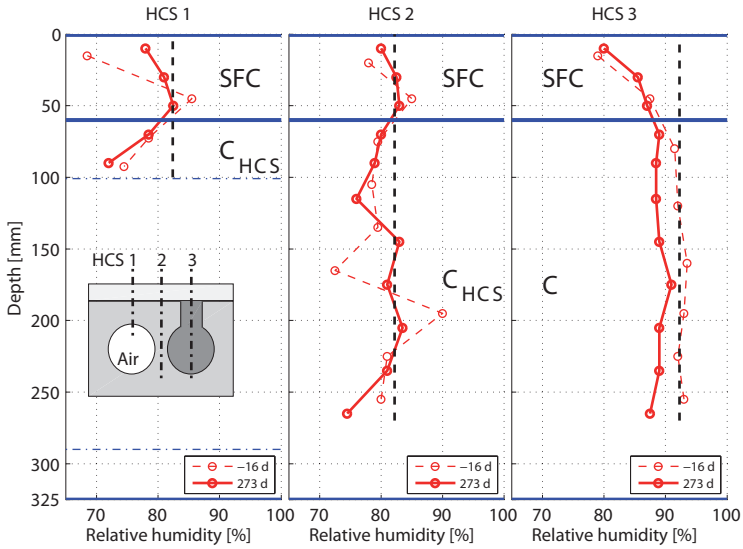

Figure 5.5: Moisture distribution determined for three separate sections of the SFC screeded HCS, with one core hole filled with material C. Sections 150-180 and 180-210 in vertical section HCS 2 were judged as outliers and therefore excluded from the estimation of future RH distribution.

see Figure 5.4. However, the maximum humidity of neither of the screeds has been reached yet. It may be expected that the humidity may increase by about 6 - 7 % RH for slab 7 and by about 2 - 3 % RH for slab 8. Incorporating these expected increases the future screed humidity in slab 7 will be underestimated by 1 - 2 % RH and by about 3 - 4 % RH in slab 8.

Comparison of the results from humidity distribution measurements with the estimated future uniform RH, the filled core, HCS3, shows about 5 - 10 % RH higher humidity level at the 10 - 30 mm level, see Figure 5.5. However, considering future upward moisture redistribution the final humidity level in the screed may increase to about 90 % RH, thus reducing the apparent overestimation to some 2 - 3 % RH. The moisture profiles determined for vertical sections HCS 1 and 2 are in addition to vertical moisture redistribution, also affected by horizontal moisture redistribution. The quantitative model is not designed for use in such cases and therefore the estimated future moisture distribution is uncertain in those two vertical sections.

Chapter 6

Discussion and conclusions

6.1 Moisture redistribution

The proposed model of moisture redistribution requires the initial moisture distribution through a screeded slab. Initial distribution may be determined before the application of flooring either in situ or under controlled conditions on samples extracted from the slab. In the study of moisture redistribution in screeded concrete slabs, samples were extracted from the slab, see Paper IV. In either case, the current status of the floor construction should be described in as much detail as possible in terms of constituent materials, layer thicknesses and moisture distribution before flooring. Furthermore, each material should be included in the determination.

In determining the moisture distribution, it may be beneficial to divide each material into a larger number of sections, since the higher resolution may reveal unexpected changes in moisture level. This high resolution would enhance the knowledge of the moisture history, thus perhaps reducing the uncertainty. In addition, by determining a number of moisture distributions in the slab it would be possible to reveal a scatter. Furthermore a rough determination of these parameters may give rise to a large uncertainty.

On the other hand, moisture may be lost during sampling by dividing the slab in too thin sections. This problem occurs as the determination of RH on thin material layers, below 10 mm, may be difficult both because of possible moisture losses during sampling and equipment installation requirements. Another limitation when deciding the possible number of sections, is the total thickness

of each material section. Each section should be treated separately, which means that mixtures of materials must be avoided.

The investigated screeded slabs were, in each case, divided into vertically discrete sections of a certain thickness. As the initial moisture distribution in the slab was unknown at the time of sampling it was determined on equally thick sections. However, as the moisture profile is very steep in certain sections the determined profile may be misleading, especially in sections close to the surfaces.

Due to limitations of the measurements techniques, a certain section size may be required to minimize uncertainties. Individual section depths could be assigned if the overall distribution is known from former measurements. If the moisture distribution is determined on material samples, these should be collected in such a way that enough material from each depth is obtained. If the moisture distribution is determined in situ using drilled in sensors, each sensor should determine the RH at the vertical midpoint of each section.

The developed quantitative model was compared with the previous model by performing a simulation of the redistribution under an impermeable seal. Initial moisture distribution to the quantitative model was obtained from a simulation of a concrete slab, with a w/c ratio of 0.65, exposed to single-sided drying at 55 % RH and 20 °C. Furthermore the calculation took into consideration moisture dependent transport properties and a sorption isotherm obtained for the material C, see section 4.2 Figure 4.6.

The moisture distribution obtained from the simulation is shown in Figure 6.1(solid curve). The input to the quantitative model was the moisture distribution obtained from the simulation and the moisture capacity for each section. Two values were assumed for the moisture capacity at the assumed RH interval, 0.1 kg/m^3 and 1.0 kg/m^3, where the humidity in the particular section is below and above respectively of the initial guess. The results from the quantitative model simulation showed that the equivalent depth increased from 0.4h in the previous model to 0.57h.

As the moisture capacity is about five to ten times higher in some parts, it is important to find those when the humidity distribution before flooring is determined. Hence, the parts at the base of a homogeneous slab have the largest effect on the result from the quantitative model. These parts should therefore be prioritized, if the number of measurements is limited.

The proposed qualitative model for estimating the moisture distribution in a screeded concrete slab fits the verifying experiments and serves as an illustration of how moisture may be redistributed inside such a slab. The quantitative estimations of moisture distribution after flooring indicate a similarity to the results obtained from the experiments. However, the humidity in the verifying screeded

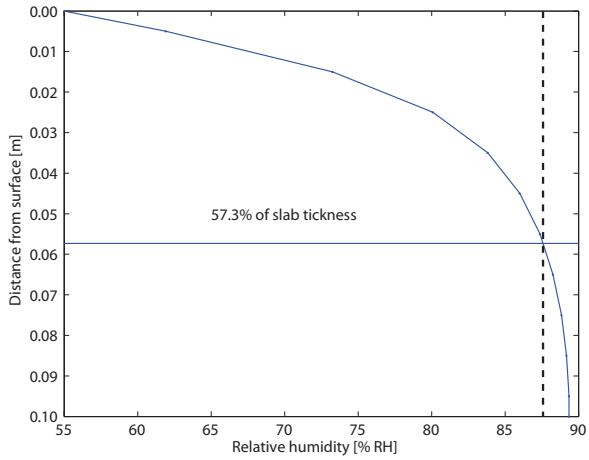

Figure 6.1: An estimation of the depth of intersection when applying the new proposed quantitative model of redistribution.

slabs has not yet been completely redistributed given the limited redistribution time.

Neither the time aspects nor possible drying are included in the model. This may lead to an overestimation of the RH level under the flooring when the screed is very dry at the time of flooring, which means a reduced risk of moisture damage. On the other hand, when the screed humidity is high, it is likely that the quantitative model underestimates the RH level under the flooring as the time needed for redistribution has a negative impact on the humidity obtained below the flooring. It may be higher than expected. The slow moisture transport in concrete is the key factor in reducing the rate of moisture redistribution. Drying from the floor construction through both flooring and slab base will favourably affect the obtained screed humidity level as the average humidity decreases, thus reducing the maximum humidity beneath the flooring.

In addition an uneven temperature distribution may affect the moisture distribution. Measurements performed on site show that the temperature, on average, is higher on the slab base than on the slab top, the report also shows that irregular temperature fluctuations are common on a construction site [50]. The lower average temperature in the floor top may have a negative effect on the humidity distribution as moisture is then transferred to the colder upper side, thus increasing the humidity.

The model uses an average moisture capacity to calculate the new moisture content at the estimated future RH distribution, see Figure 6.2.

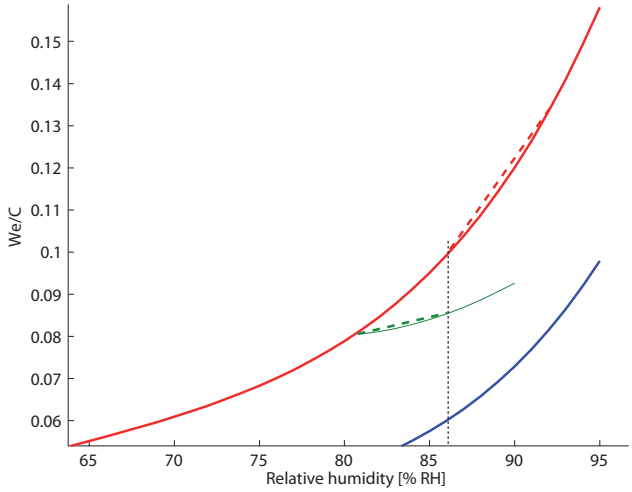

Figure 6.2: The average moisture capacity shown for two separate sections of a screeded slab, one for the desorption isotherm (red dashed line) and one for the scanning curve (green dashed line). The uniform RH after redistribution is shown as a vertical dotted line.

It is possible to develop software which is able to estimate the moisture distribution underneath flooring according to the proposed quantitative model. However, additional data on sorption isotherms for concrete mixtures and screed compounds, not included in this research, needs to be further investigated. The software would require a model for estimating scanning curves for different materials, as such are not available for all expected conditions.

Sorption isotherms and scanning curves

The sorption balance is very useful for determining sorption isotherms of cement-based materials [43, 51, 52]. Besides reduced labour costs, the speed of determining one desorption and absorption isotherm is increased by a factor of 10 compared with the previously used climate chamber method [53, 54]. Such high speed isotherm determination is beneficial as uncertainties arising from hydration are reduced. In addition, sorption balances are accurate enough to perform scanning curve investigations. The small samples of concrete and mortar are not representative and require chemical analysis of each sample. Sampling from dried slabs gave the 2^{nd} desorption isotherm. Testing is undertaken in a carbonate free environment thus preventing carbonation. However, one drawback is the high

initial cost of the sorption balance.

In Paper III, several scanning curves were presented for concrete, mortar and one self-levelling flooring compound. All these scanning curves were investigated by subjecting the material sample to a linearly increasing/decreasing RH in a sorption balance. This method has previously been used in [43]. However, small but significant time lag effects occurred as a consequence of the slow moisture exchange between the passing gas stream and the samples. These were minimized by linearly distributing the error originating from the start and the end levels on the scanning curve. After this linear error distribution the time lag effects were reduced.

The small time lag effect may be further reduced by using an RH step change sequence for evaluating scanning curves. In this way there is a possibility to extrapolate each step's final mass instead of using linearly distributed errors, thus further reducing possible time lag effects.

Results from the repeated scanning sorption isotherm investigations indicate that the moisture content is recovered when returning to the desorption isotherm after performing one scanning curve loop.

Redistribution of moisture after early drying

The redistribution of moisture was determined by inserting probes in plastic tubes perpendicular to the moisture flow. Since the plastic tubes were present during drying and later redistribution they affected the moisture flow. However, by inserting the probes at various depths from the surface 80 mm into the concrete cylinder, the flow of moisture at the centre part was left undisturbed. Installing RH probes vertically from the top would certainly hinder moisture flow as the probe itself would obstruct moisture transport during drying and redistribution. The obstruction leads to a higher RH than if measurements are performed horizontally from the side, since moisture accumulates below the probe. A larger opening facing the concrete from the top will have a greater impact on moisture transport. It is easily recognized that all desiccation would cease if the opening occupied the specimens' top surface completely. Instead, a redistribution would start. Another option of installation is to insert the RH probe from the cylinder base. This would imply that the material below the measurement point would be replaced by the plastic tube. This loss of material would also mean a moisture source loss. By performing the measurements from the side the moisture flow is disturbed only in the immediate vicinity of the tube opening.

When RH probes are installed perpendicular to the moisture flow other errors are introduced see Figure 6.3. One error is dependent on the position with

reference to the moisture distribution. The RH probe determines the humidity of the air in the sealed tube, and this air humidity is determined by the concrete's surface humidity facing the opening. Since the vertical opening is not sealed it will allow a moisture flow, a redistribution from humid surface areas to drier areas. The redistribution occurs through the surgical tape and the air in the tube. This means that the humidity in the air will end up at a level somewhere between the humidity at the bottom and the top of the tube opening. This error is dependent on the installation location with respect to the moisture distribution. A probe installed at a shallow depth faces a distribution that varies a lot with depth, while a probe installed deeper faces a moisture distribution with considerably less variation. It also means that a shallow probe will show a higher RH than is actually the case in a drying situation. However, when a seal is attached to the surface the depth dependent error decreases with time. After the moisture has been completely redistributed and the moisture flow has ceased this error no longer exists.

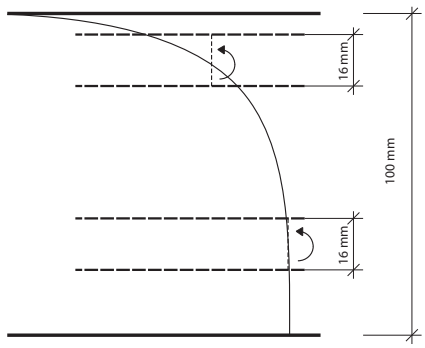

Figure 6.3: Two probes installed at different depths in a concrete specimen. Dashed lines represent the concrete surface facing the probe. The arrow indicates the direction of redistribution.

A flooring on a concrete slab is typically not completely impermeable, which means that drying continues after installation. In a less dense flooring material the humidity load on the adhesive is less than estimated by using the quantitative model of moisture redistribution. If the flooring is installed by using a water soluble adhesive a certain wetting of the concrete occurs, and this increases the RH load on the adhesive. These two factors affect the level of humidity exposure below the flooring and the duration of the estimated humidity.

The outcome of the study may have been different if drying had been performed at a lower RH. Additionally the type of cement used in the concrete specimens was rapid hardening and this may also contribute to the small differences achieved between the two drying treatments. Rapid hardening cement hydrates much faster than an ordinary Portland cement, hence possibly diminishing the expected difference between the two drying treatments.

6.2 Critical limit for ion transport

Potassium ion distribution was determined on mortar specimens subjected to a drying treatment described in Paper IV. The drying treatment generated a moisture distribution obtained through an equivalent moisture history. This is an important issue, as the proportion of empty capillaries is not consistent if the moisture history differs within the material, due to the hysteresis exhibited by the sorption isotherm. The moisture content at a particular RH is higher if it results from a decrease in humidity (drying) than if it results from an increase in humidity (wetting). Furthermore, the maximum moisture content at a particular RH is attained by drying a virgin concrete never exposed to any prior drying treatment. In addition the drying treatment applied to the sample should preferably not generate a non-uniform ion distribution, since it may cause diffusion, especially at high humidities.

In efforts to find the critical limit for ion transport it is vital to achieve the highest possible moisture content for the investigated humidity. In any other case the critical humidity would be underestimated, hence achieving a higher critical humidity than the ”true” one. If the investigated material exhibits a variation in moisture content, the achieved critical limit would be uncertain, regardless of a uniform RH distribution. The inconsistent moisture content would affect the ratio between the filled and emptied capillaries. This means that there would be a reduced opportunity for ion transport.

6.3 Other aspects

The moisture flow resistance of the flooring material and the slab material, influences the humidity increase achieved by the redistributed moisture. This increase becomes larger if the flooring material exhibits a higher moisture flow resistance than the slab material. Such floor constructions are commonly utilized in the construction industry. It is for instance common to apply a PVC flooring to a

high w/c ratio concrete slab, with the risk of severely increasing the humidity under the flooring. The low moisture transport resistance of high w/c ratio concrete enables a large moisture flow towards the flooring. The moisture flow allowed through the flooring material is far lower. This means that the inflow of water is higher than the out flow, hence increasing the humidity.

Redistributed moisture would have a much smaller impact on the humidity under a PVC flooring given a low w/c ratio concrete in the slab. The difference in moisture flow resistance between a low w/c ratio concrete and a PVC flooring is of equal magnitude. This means that the flow of moisture to the flooring and the flow from it is also of equal magnitude. Therefore the humidity increase in such a case is rather moderate because of redistributed moisture.

The suggested model of moisture redistribution presented in section 3.3, takes into account the effect of hysteresis. This changes the point of intersection between the moisture distribution prior to flooring installation and that after completion of redistribution. The consequence is that the point of intersection is located deeper than the previously suggested 0.4 of the slab thickness. This is clearly shown in the results in Paper VI where the point of intersection is located at about 0.5 - 0.55 of the slab thickness. It must however be borne in mind that this result was obtained when the slab was completely sealed at both the bottom and the top, which is seldom the case in practice.

Unsaturated concrete exists in both outdoor and indoor structures. Ion movement in these structures may have an adverse impact on the durability. For instance, chloride ion movement in unsaturated low w/c ratio concrete may occur in submerged constructions like caissons and concrete columns supporting bridges. Accumulation of chlorides may initiate corrosion of the reinforcement, hence reducing the durability. Another example where unsaturated concrete occurs, is the splash zone in marine constructions where the moisture conditions change frequently. Also in this application the chloride ion is the adverse species. In addition, onshore constructions like the walls of a swimming pool contain unsaturated concrete, with a potential of chloride transport with the risk of reinforcement corrosion.

Furthermore, unsaturated concrete is more or less the natural condition in indoor applications. Ion transport may in this case contribute to a reduction in the durability of a flooring. The alkali ions in concrete contribute to material deterioration when redistributed moisture conveys them to the adhesive. The adhesive is degraded and the bond between the concrete and flooring is reduced. Apart from the disagreeable odour, the degradation products, VOC, they are believed to have an adverse effect on peoples' health.

Chapter 7

Future research

The results from this research have raised a number of questions that need to be investigated to develop the proposed models further.

Additional input, such as sorption isotherms including scanning curves for other concrete mixes and screeds are needed to decrease uncertainties of the proposed model. Desorption isotherms determined for samples extracted from shallow parts of concrete showed a decrease with time in their ability to bind moisture by absorption. Samples extracted from deeper lying parts also showed a decrease in the ability to bind moisture by absorption. These two findings may have an impact on moisture redistribution.

As the sorption isotherm is temperature dependent and low temperatures regularly occur during construction, additional sorption isotherms should be determined for temperatures other than 20 °C.

The model does not take into consideration time lag effects and drying that may occur through the flooring material and an open base surface. Drying will decrease the humidity beneath flooring, thus reducing the risk of moisture related damage.

A detailed analysis of the uncertainties involved and the way in which they may affect the estimated maximum humidity level is not performed in this work. However, uncertainties originating from a lot of sources are briefly mentioned in the next four paragraphs.

First of all, the uncertainty involved in RH determinations of each section will affect the overall uncertainty. However, when a complete distribution throughout an entire screeded slab is determined, the overall uncertainty in moisture distribution decreases. Sections may be regarded as outliers, disqualifying

them from further analysis.

Secondly, by performing a detailed moisture distribution determination throughout the entire slab by subdividing it into many horizontal sections, a lower uncertainty may be obtained. The converse, a higher uncertainty, will follow if a non-sufficient, poor, low resolution, or incomplete moisture distribution determination is performed. In such a case it is not possible to disregard outliers.

Thirdly, possible non-uniform temperature distributions may also add to the uncertainty, since such are not included in the model. Such a non-uniform temperature distribution will redirect moisture flow from warmer towards colder sections inside the screeded slab, with a non-uniform moisture distribution as the result.

A fourth source of uncertainty is drying that may occur through the slab base and flooring. Further drying will reduce the humidity level underneath the flooring and thus reduce the maximum humidity beneath the flooring.

The magnitude of the above uncertainties needs to be further investigated in future research. Some of the above sources of uncertainty affect the maximum humidity more than others. Some may even possibly be disregarded.

Bibliography

[1] L.-O. Nilsson. Moisture measurements Excess moisture in concrete slabs on grade. Drying and measurement methods. (in Swedish). Technical Report TVBM-3008, Div Building Materials, Lund University, 1979.

[2] RBK. *Moisture measurement in concrete (in Swedish)*. Sveriges Byggindustrier, Stockholm, Manual 3^{rd} edition, 2001.

[3] E.O. Kraemer. *A treatise on Physical Chemistry*. Van Nostrand, New York, 1931.

[4] J.W. McBain. An explanation of hysteresis in the hydration and dehydration of gels. *Journal of American Chemical Society*, 57:699–700, 1935.

[5] S. Diamond and K.O. Kjellsen. Resolution of fine fibrous C-S-H in backscatter SEM examination. *Cement and Concrete Composites*, 28(2):130–132, 2006.

[6] R.F. Feldman and P.J. Sereda. A new model for hydrated portland cement and its practical implications. *Engineering Journal*, 53(8-9):53–59, 1970.

[7] H.M. Jennings. A model for the microstructure of calcium silicate hydrate in cement paste. *Cement and Concrete Research*, 30(1):101–116, 2000.

[8] I.G. Richardson. The calcium silicate hydrates. *Cement and Concrete Research*, 38(2):137–158, 2008.

[9] V. Baroghel-Bouny. Water vapour sorption experiments on hardened cementitious materials. Part I: Essential tool for analysis of hygral behaviour and its relation to pore structure. *Cement and Concrete Research*, 37(3):414–437, 2007.

[10] I. Langmuir. The adsorption of gases on plane surfaces of glass, mica and platinum. *Journal of the American Chemical Society*, 40:1361–1403, JUL-DEC 1918.

[11] S. Brunauer, P.H. Emmett, and E. Teller. Adsorption of gases in multimolecular layers. *Journal of the American Chemical Society*, 60 (2):309–319, 1938.

[12] R.W. Dent. A multilayer theory for gas sorption. Part I. Sorption of a Single gas. *Textile Research Journal*, 47(3):188–199, 1977.

[13] T.C. Powers and T.L. Brownyard. Studies of the physical properties of hardened portland cement paste, bulletin 22. *Res. Lab. of Portland Cement Association, Skokie, IL, U.S.A., reprinted from Journal of the American Concerete Institute (Proc.), vol. 43*, pages 101–132, 249–336, 469–504, 549–602, 669–712, 845–880, 933–992, 1947.

[14] T. Young. An essay on the cohesion of fluids. *Philosophical Transactions of the Royal Society of London*, 95:65–87, 1805.

[15] P. S. Laplace. *Traité de mécanique céleste*, chapter Supplément au dixième livre du Traité de mécanique céleste, Sur l'action capillaire, pages 1–67. Courcier, Paris, 1806.

[16] P. S. Laplace. *Traité de mécanique céleste*, chapter Supplément au dixième livre du Traité de mécanique céleste, Supplément a la théorie de l'action capillaire, pages 1–78. Courcier, Paris, 1807.

[17] W. Thomson. On the equilibrium of vapour at a curved surface of liquid. In *Proceedings of the Royal Society of Edinburgh*, volume 42, 1871.

[18] D.H. Everett. Adsorption hysteresis. In E.A. Flood, editor, *The Solid-Gas interface Vol. 2*, pages 1055–1113. Marcel Dekker, New York, 1967.

[19] P.C. Carman and P. le R. Malherbe. Diffusion and Flow of Gases and Vapours through Micropores. II. Surface Flow. *Proceedings of the Royal Society of London. Series A. Mathematical and Physical Sciences*, 203(1073):165–178, 1950.

[20] R.M. Barrer and J.A. Barrie. Sorption and Surface Diffusion in Porous Glass. *Proceedings of the Royal Society of London. Series A. Mathematical and Physical Sciences*, 213(1113):250–265, 1952.

[21] P.C. Carman. Diffusion and Flow of Gases and Vapours through Micropores. IV. Flow of Capillary Condensate. *Proceedings of the Royal Society of London. Series A. Mathematical and Physical Sciences*, 211(1107):526–535, 1952.

[22] E. Samson, J. Marchand, K. A. Snyder, and J. J. Beaudoin. Modeling ion and fluid transport in unsaturated cement systems in isothermal conditions. *Cement and Concrete Research*, 35(1):141–153, 2005.

[23] A.T.C. Guimar aes, M.A. Climent, G. de Vera, F.J. Vicente, F.T. Rodrigues, and C. Andrade. Determination of chloride diffusivity through partially saturated portland cement concrete by a simplified procedure. *Construction and Building Materials*, 25(2):785 – 790, 2011.

[24] M.A. Climent, G. de Vera, J.F. López, E. Viqueira, and C. Andrade. A test method for measuring chloride diffusion coefficients through nonsaturated concrete: Part I. The instantaneous plane source diffusion case. *Cement and Concrete Research*, 32(7):1113 – 1123, 2002.

[25] G. de Vera, M.A. Climent, E. Viqueira, C. Antón, and C. Andrade. A test method for measuring chloride diffusion coefficients through partially saturated concrete. Part II: The instantaneous plane source diffusion case with chloride binding consideration. *Cement and Concrete Research*, 37(5):714 – 724, 2007.

[26] M.A. Climent, G. de Vera, J.F. López, C. Garcia, and C. Andrade. Transport of chlorides through non-saturated concrete after an initial limited chloride supply. In Andrade, C and Kropp, J, editor, *2^{nd} International RILEM Workshop on testing and modelling the chloride ingress into concrete*, volume 19 of *RILEM Proceedings*, pages 173–187, 2000.

[27] A.V. Saetta, R.V. Scotta, and R.V. Vitaliani. Analysis of chloride diffusion into partially saturated concrete. *ACI Materials Journal*, 90(5):441–451, SEP-OCT 1993.

[28] O. Francy. *Modélisation de la pénétration des ions clorures dans les mortier partiellement saturés en eau*. PhD thesis, Université Paul Abatier, 1998.

[29] E.P. Nielsen and M.R. Geiker. Chloride diffusion in partially saturated cementitious material. *Cement and Concrete Research*, 33(1):133–138, 2003.

[30] U. Angst, B. Elsener, R. Myrdal, and Ø. Vennesland. Diffusion potentials in porous mortar in a moisture state below saturation. *Electrochimica Acta*, 55(28):8545 – 8555, 2010.

[31] T.Q. Nguyen. *Modélisations physico-chimiques de la pénétration des ions chlorures dans les matériaux cimentaires*. PhD thesis, L'ecole nationale des ponts et chaussees, 2007.

[32] T.Q. Nguyen, J. Petkovic, P. Dangla, and V. Baroghel-Bouny. Modelling of coupled ion and moisture transport in porous building materials. *Construction and Building Materials*, 22(11):2185–2195, 2008.

[33] P. Castro, O.T. De Rincon, and E.J. Pazini. Interpretation of chloride profiles from concrete exposed to tropical marine environments. *Cement and Concrete Research*, 31(4):529–537, 2001.

[34] L.-O. Nilsson. A numerical model for combined diffusion and convection of chloride in non-saturated concrete. In Andrade, C and Kropp, J, editor, *2nd International RILEM Workshop on testing and modelling the chloride ingress into concrete*, volume 19 of *RILEM Proceedings*, pages 261–275, 2000.

[35] E. Bastidas-Arteaga, A. Chateauneuf, M. Sánchez-Silva, Ph. Bressolette, and F. Schoefs. A comprehensive probabilistic model of chloride ingress in unsaturated concrete. *Engineering Structures*, 33(3):720–730, 2011.

[36] H. Wengholt Johnsson. *Chemical emissions from flooring systems - the effect of different concrete grades and moisture loads (in Swedish)*. Licentiate thesis, Chalmers University of Technology, 1995.

[37] A. Anderberg. *Studies of moisture and alkalinity in self-levelling flooring compounds*. PhD thesis, Div of Building Materials, Lund University, 2007.

[38] G. Hedenblad and L.-O. Nilsson. Critical moisture levels of some building materials - preliminary study (in Swedish). Technical Report TVBM-3028, Div of Building Materials, Lund University, 1987.

[39] T.C. Powers. A discussion of cement hydration in relation to the curing of concrete. In *Proceedings 27*, pages 178–188, Washington, D.C., 1947. Highway Research Board.

[40] M. Gerstig and L. Wadsö. A method based on isothermal calorimetry to quantify the influence of moisture on the hydration rate of young cement pastes. *Cement and Concrete Research*, 40(6):867–874, 2010.

[41] H. H. Willems and K. B. Van Der Velden. A gravimetric study of water vapour sorption on hydrated cement pastes. *Thermochimica Acta*, 82(1):211–220, 1984.

[42] l. Zhang and F.P. Glasser. Critical examination of drying damage to cement pastes. *Advances in cement research*, 12(2):79–88, 2000.

[43] A. Anderberg and L. Wadsö. Moisture in self-levelling flooring compounds. Part II. Sorption isotherms. *Nordic Concrete Research*, 32(2):16–30, 2004.

[44] L. Greenspan. Humidity fixed point of binary saturated aqueous solutions. *Journal of research of the national bureau of standards - A. Physics and Chemistry*, 81 A(1):89–96, 1977.

[45] A. Anderberg and L. Wadsö. Moisture in self-levelling flooring compounds. Part I. Water vapour diffusion coefficients. *Nordic Concrete Research*, 32(2):3–15, 2004.

[46] A. Sjöberg. *Secondary emissons from concrete floors with bonded flooring materials - effects of alkaline hydrolysis and stored decomposition products*. PhD thesis, Chalmers University of Technology, 2001.

[47] A. Sjöberg and O. Ramnäs. An experimental parametric study of VOC from flooring systems exposed to alkaline solutions. *Indoor Air*, 17(6):450–457, 2007.

[48] L.-O. Nilsson and J. Aavik. Drying of residual moisture in vaccuum treated concrete floors on ground on thermal insulation. Part C: Drying of residual moisture - Validation in a laboratory. Part D: Drying of residual moisture - In situ measurements(in Swedish). Technical Report P-93:13, 1993.

[49] A. Sjöberg and L.-O. Nilsson. Moisture measurements in heated concrete floors. Part II: Impervious floorings (in Swedish). Technical Report TVBM-3140, Div of Building Materials, Lund University, 2008.

[50] M. Åhs. Remote monitoring and logging of relative humidity in concrete. In *Proceedings of the 7th symposium on building physics in the nordic countries*, volume 1, pages 181–187, Reykjavik, Iceland, 2005. The icelandic building research institute.

[51] B. Johannesson and M. Janz. Test of four different experimental methods to determine sorption isotherms. *Journal of Materials in Civil Engineering*, 14(6):471–477, 2002.

[52] R. M. Espinosa and L. Franke. Inkbottle pore-method: Prediction of hygroscopic water content in hardened cement paste at variable climatic conditions. *Cement and Concrete Research*, 36(10):1954–1968, 2006.

[53] V. Baroghel-Bouny and T. Chaussadent. Pore structure and moisture properties of cement-based systems from water vapour sorption isotherms. In Diamond, S and Mindess, S and Glasser, FP and Roberts, LW and Skalny, JP and Wakeley, LD, editor, *Microstructure of Cement-Based Systems/Bonding and Interfaces in Cementitious Materials*, volume 370 of *Materials Research Society Symposium Proceedings*, pages 245–254, 1995.

[54] L. Ahlgren. *Moisture fixation in porous building materials (in Swedish)*. PhD thesis, Div of Building Materials, Lund University, 1972.

Appendix

Ion redistribution in mortar specimens

Ion distribution in the mortar specimens is shown in the following figures. The potassium content is shown on the y-axis and the x-axis represents the average position of the SEM-EDS analysis image, in mm, with reference to the surface subjected to the 2^{nd} drying (the right hand side in each diagram). The average potassium content in each image is represented by the thin solid curve and is quantified as the wt.-%. The average content through half of the specimen, right and left, is shown as a solid horizontal line. The midpoint is at around -14 mm, depending on the specimen thickness. The error bars represent the standard deviation of the potassium content at each image (point).

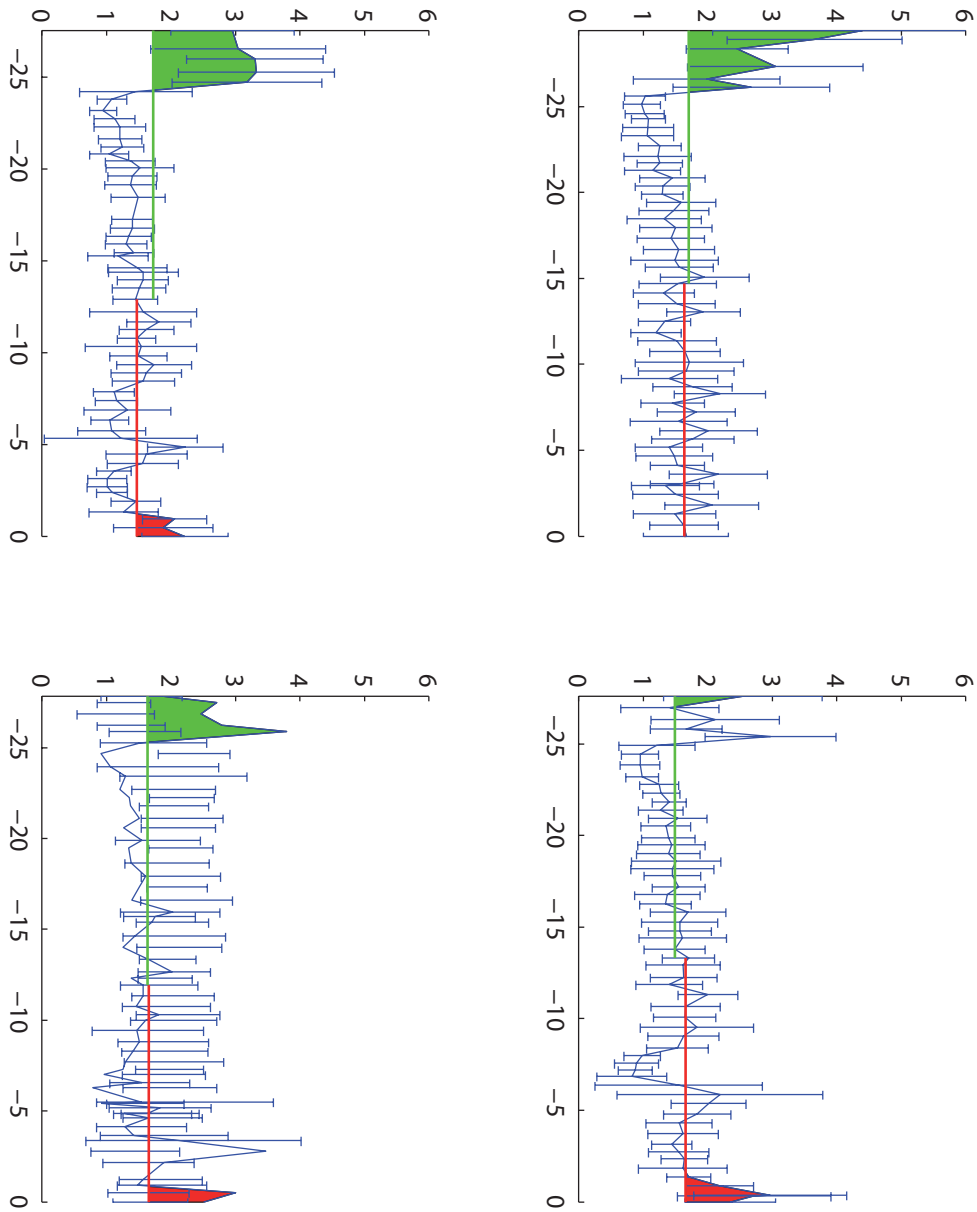

Figure A.1: Standard deviation of the potassium content at each image(point) of the w/c 0.65 mortar conditioned to 78% RH before 2nd drying.

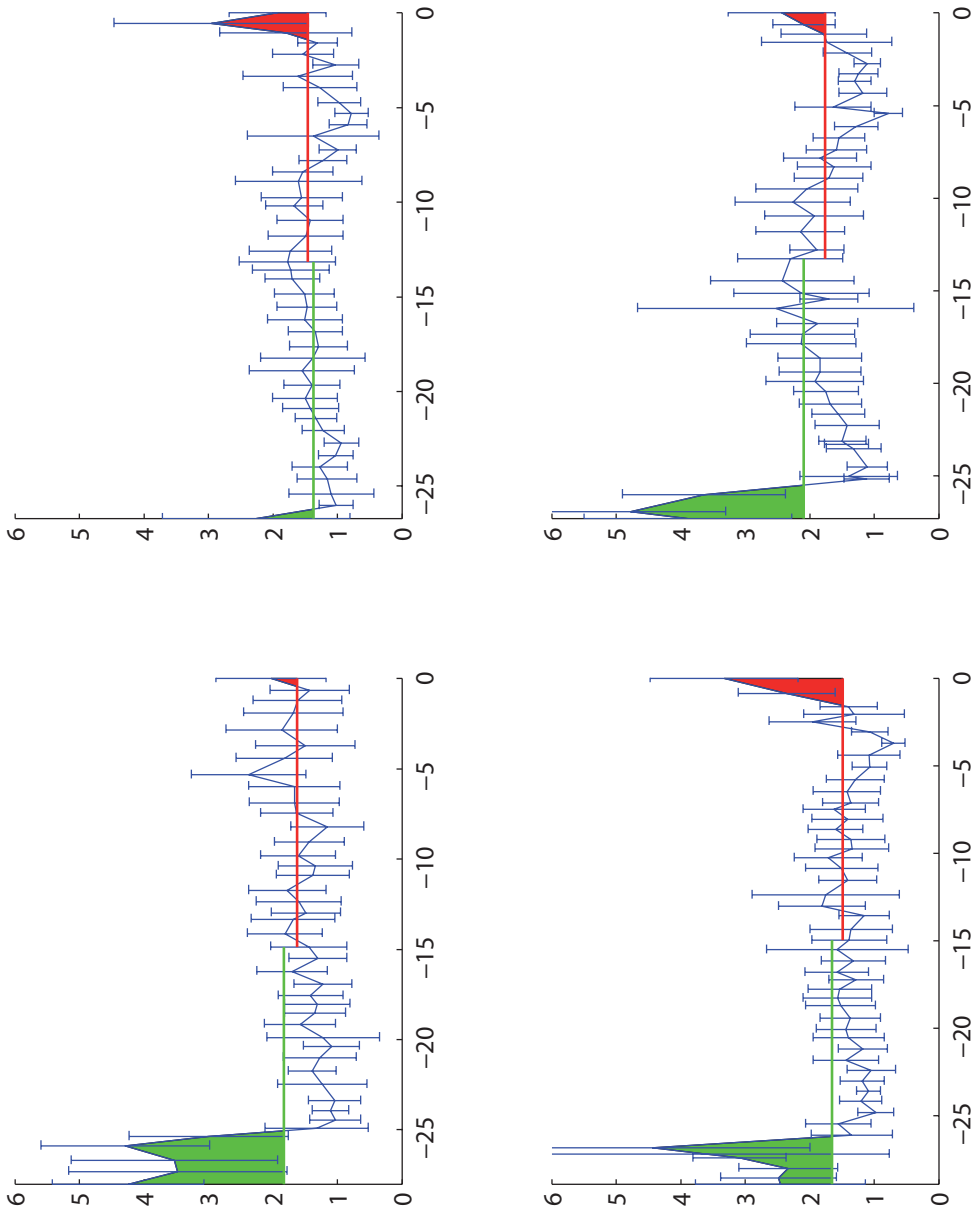

Figure A.2: Standard deviation of the potassium content at each image(point) of the w/c 0.65 mortar conditioned to 83% RH before 2nd drying.

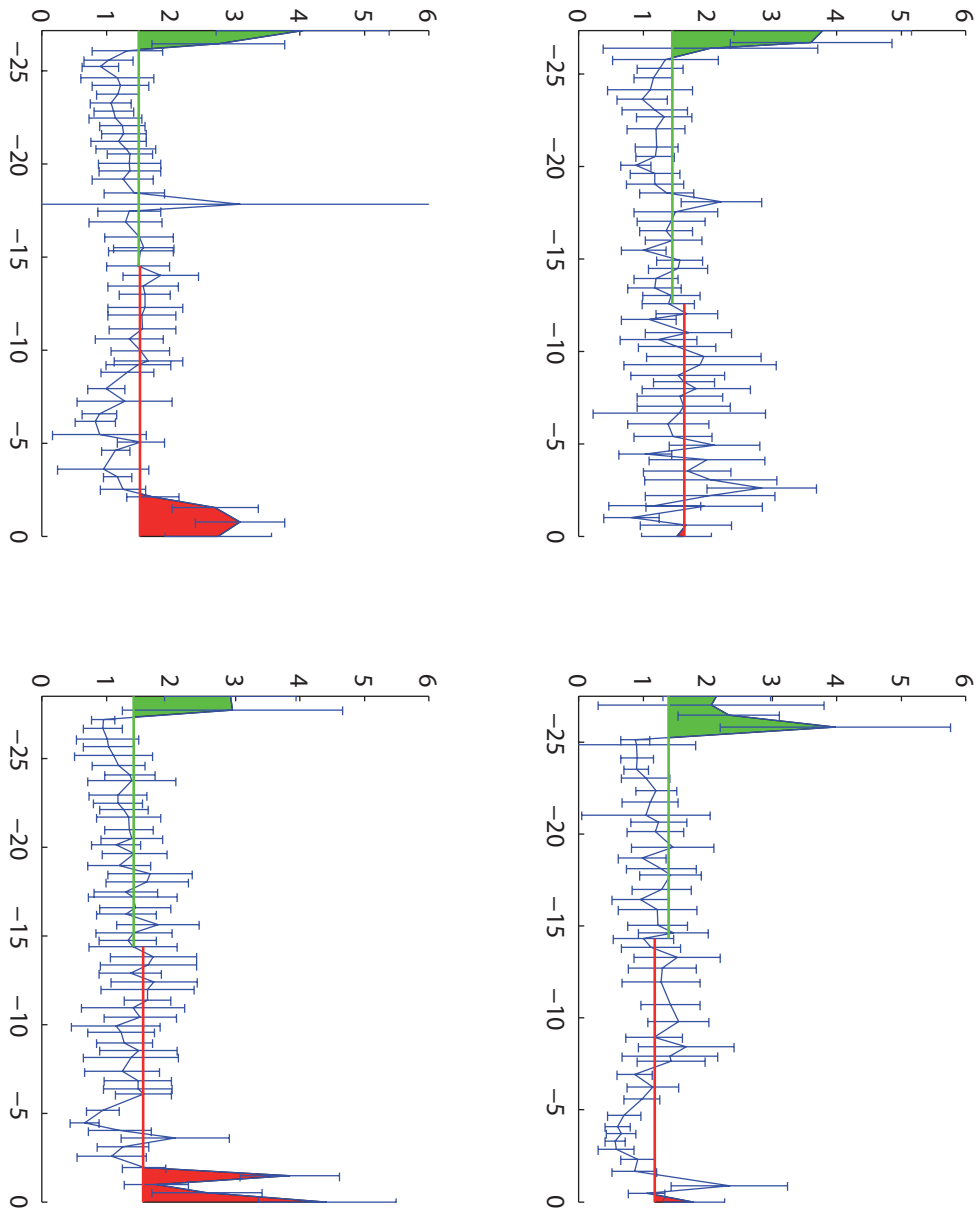

Figure A.3: Standard deviation of the potassium content at each image(point) of the w/c 0.65 mortar conditioned to 85% RH before 2nd drying.

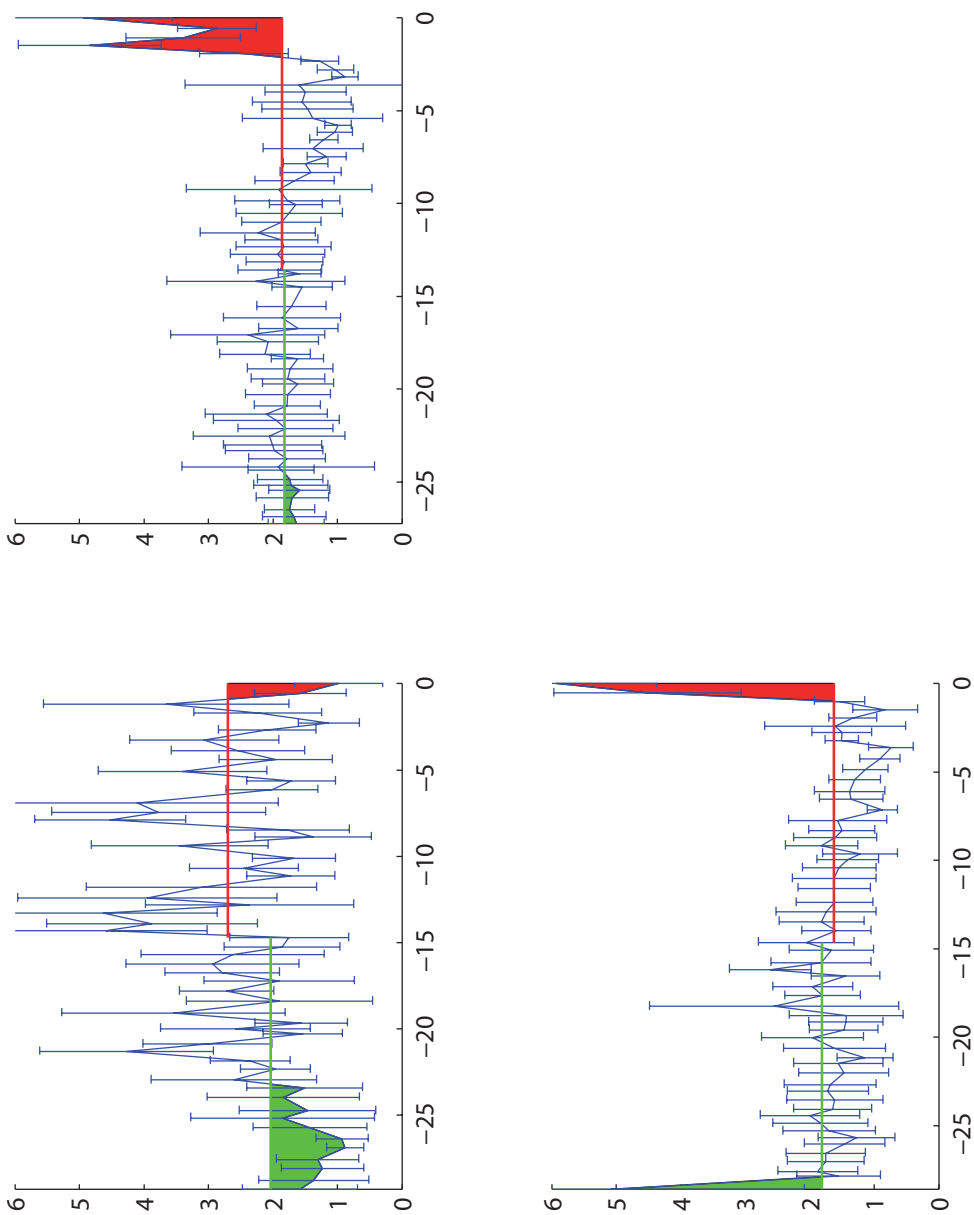

Figure A.4: Standard deviation of the potassium content at each image(point) of the w/c 0.65 mortar conditioned to 93% RH before 2nd drying.

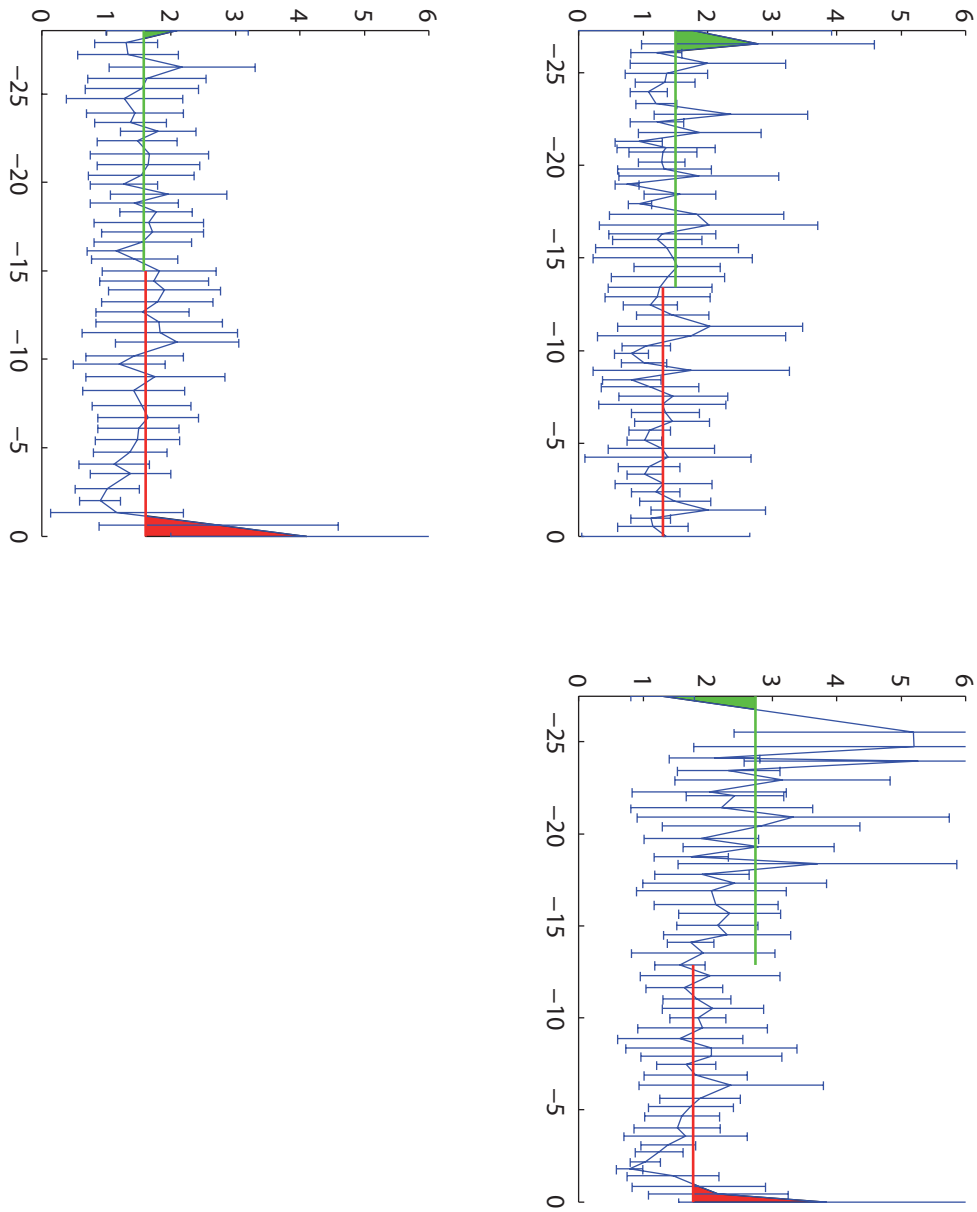

Figure A.5: Standard deviation of the potassium content at each image(point) of the w/c 0.4 mortar conditioned to 91% RH before 2nd drying.

LUND UNIVERSITY